Sezione ROMA III
Via della Vasca Navale 84
I-00146 Roma, Italy

INFN-RM3 98/2
September 1998

Power corrections in the longitudinal and transverse structure functions of proton and deuteron[a]

G. Ricco[(a,b)], S. Simula[(c)] and M. Battaglieri[(b)]

[(a)]Dipartimento di Fisica, Universitá di Genova
Via Dodecanneso 33, I-16146, Genova, Italy
[(b)]Istituto Nazionale di Fisica Nucleare, Sezione di Genova
Via Dodecanneso 33, I-16146, Genova, Italy
[(c)]Istituto Nazionale di Fisica Nucleare, Sezione Roma III
Via della Vasca Navale 84, I-00146 Roma, Italy

Abstract

Power corrections to the Q^2 behaviour of the low-order moments of both the longitudinal and transverse structure functions of proton and deuteron have been investigated using available phenomenological fits of existing data in the Q^2 range between 1 and 20 $(GeV/c)^2$. The Natchmann definition of the moments has been adopted for disentangling properly target-mass and dynamical higher-twist effects in the data. The leading twist has been treated at next-to-leading order in the strong coupling constant and the effects of higher orders of the perturbative series have been estimated using a renormalon-inspired model. The contributions of (target-dependent) multiparton

[a]**To appear in Nuclear Physics B.**

correlations to both $1/Q^2$ and $1/Q^4$ power terms have been determined in the transverse channel, while the longitudinal one appears to be consistent with a pure infrared renormalon picture in the whole Q^2-range between 1 and 20 $(GeV/c)^2$. Finally, the extracted twist-2 contribution in the deuteron turns out to be compatible with the hypothesis of an enhanced d-quark parton distribution at large x.

1 Introduction

The experimental investigation of deep-inelastic lepton-hadron scattering has provided a wealth of information on the occurrence of Bjorken scaling and its violations, giving a decisive support to the rise of the parton model and to the idea of asymptotic freedom. Quantum Chromodynamics (QCD) has been thereby proposed as the theory describing the logarithmic violations to scaling in the asymptotic region and its predictions at leading (LO) and next-to-leading (NLO) orders have been nicely confirmed by the experiments. However, in the pre-asymptotic region the full dependence of the hadron structure functions on the squared four-momentum transfer, $Q^2 \equiv q \cdot q$, is affected also by power corrections, which can originate from non-perturbative physics and are well beyond the predictive power of perturbative QCD. An important tool for the theoretical investigation of the Q^2 behaviour of the structure functions is the Operator Product Expansion (OPE): the logarithmic scale dependence is provided by the so-called leading twist operators, which in the parton language are one-body operators whose matrix elements yield the contribution of the individual partons to the structure functions. On the contrary, power corrections are associated to higher-twist operators which measure the relevance of correlations among partons (see, e.g., [1]).

In case of unpolarised inelastic electron scattering the nucleon response is described by two independent quantities: the transverse $F_2^N(x,Q^2)$ and the longitudinal $F_L^N(x,Q^2)$ structure functions, where $x \equiv Q^2/2M\nu$ is the Bjorken variable, with M and ν being the nucleon mass and the energy transfer in the target rest frame. Systematic measurement of the transverse structure function of the nucleon, $F_2^N(x,Q^2)$, (more precisely, of the proton and the deuteron [2, 3, 4, 5, 6]) have been carried out in the kinematical range $10^{-4} \lesssim x \lesssim 1$ and for Q^2 values up to several hundreds of $(GeV/c)^2$; thus, various phenomenological fits of the data sets are presently available, like those of Refs. [2, 7, 8]. As for the longitudinal to transverse (L/T) cross section ratio, $R_{L/T}^N(x,Q^2) \equiv \sigma_L^N(x,Q^2)/\sigma_T^N(x,Q^2)$, the experimentally investigated kinematical range is $0.0045 \lesssim x \lesssim 0.7$ and $1 \lesssim Q^2\ (GeV/c)^2 \lesssim 70$ [4, 5, 6, 9]; however, the sparse and still fluctuating data are not yet sufficient to put significative constraints on the phenomenological fits (see Refs. [10, 11]), particularly in the low-x region ($x \lesssim 0.3$).

Various analyses of power-suppressed terms in the world data on both $F_2^N(x,Q^2)$ and $F_L^N(x,Q^2)$ structure functions have been already carried out; they are based either on the choice of a phenomenological ansätz [12, 13] or on renormalon-inspired models [14, 15], adopting for the leading twist the LO or NLO approximations. Very recently, also the effects of the next-to-next-to-leading order ($NNLO$) have been investigated on $F_2^N(x,Q^2)$ and $R_{L/T}^N(x,Q^2)$ [16] as well as on the parity-violating structure function $xF_3^N(x,Q^2)$ [17], measured in the neutrino and antineutrino scattering off iron by the $CCFR$ collaboration [18]. Present analyses at $NNLO$ seem to indicate that power corrections in $F_2^N(x,Q^2)$, $R_{L/T}^N(x,Q^2)$ and $xF_3^N(x,Q^2)$ can be quite small. However, in such analyses the highest value of x is typically limited at $\simeq 0.75$ and also the adopted Q^2 range is quite restricted ($Q^2 \gtrsim 5 \div 6\ (GeV/c)^2$ at $x \simeq 0.75$) in order to avoid the nucleon-resonance region; therefore, in such kinematical conditions the power corrections represent always a small fraction of the leading-twist term (corrected for target-mass effects). Furthermore, when power corrections are

investigated in a narrow Q^2-window, it is clear that variations of the logarithmic dependence of the leading twist can easily simulate a small power-like term as well as a significative sensitivity to the higher-twist anomalous dimensions cannot be easily achieved.

We point out that the smallness of the sum of the various dynamical higher-twists does not imply the smallness of its individual terms and therefore the question whether present data are compatible with an alternate-sign twist expansion is still open. To answer this question, we extend in this paper the range of values of Q^2 down to $Q^2 \simeq 1$ $(GeV/c)^2$ in order to enhance the sensitivity to power-like terms. For such low values of Q^2 we expect that the effects of target-dependent higher twists (i.e., multiparton correlations) should show up, thanks also to the contributions of the nucleon-resonance region and the nucleon elastic peak. The inclusion of the nucleon-resonance region is clearly worthwhile also because of parton-hadron duality arguments (see, e.g., Ref. [19]).

In this paper we analyse the power corrections to the Q^2 behaviour of the low-order moments of both the longitudinal and transverse structure functions of proton and deuteron using available phenomenological fits of existing data in the Q^2 range between 1 and 20 $(GeV/c)^2$, including also the $SLAC$ proton data of Ref. [3] covering the region beyond $x \simeq 0.7$ up to $x \simeq 0.98$. The Natchmann definition of the moments is adopted for disentangling properly target-mass and dynamical higher-twist effects in the data. The leading twist is treated at NLO in the strong coupling constant and, as far as the transverse channel is concerned, it is extracted simultaneously with the higher-twist terms from the data. The effects of higher orders of the perturbative series are estimated adopting the infrared (IR) renormalon model of Ref. [14], containing both $1/Q^2$ and $1/Q^4$ power-like terms. It turns out that the longitudinal and transverse data cannot be explained simultaneously by a renormalon contribution only; however, we will show that in the whole Q^2 range between 1 and 20 $(GeV/c)^2$ the longitudinal channel appears to be consistent with a pure IR-renormalon picture, adopting strengths which are not inconsistent with those expected in the naive non-abelianization (NNA) approximation [15] and agree well with the results of a recent analysis [17] of the $CCFR$ data [18] on $xF_3^N(x,Q^2)$. Then, after including the $1/Q^2$ and $1/Q^4$ IR-renormalon terms as fixed by the longitudinal channel, the twist-4 and twist-6 contributions arising from multiparton correlations are phenomenologically determined in the transverse channel and found to have non-negligible strengths with opposite signs. It is also shown that our determination of multiparton correlation effects in $F_2^N(X,Q^2)$ is only marginally affected by the specific value adopted for the strong coupling constant at the Z-boson mass, at least in the range between $\simeq 0.113$ and $\simeq 0.118$. Finally, an interesting outcome of our analysis is that the extracted twist-2 contribution in the deuteron turns out to be compatible with the enhancement of the d-quark parton distribution recently proposed in Ref. [16].

The paper is organised as follows. In the next Section the main features of the OPE, the NLO approximation of the leading twist and the usefulness of the Natchmann definition of the moments are briefly reminded. In Section 3 our procedure for the evaluation of the *experimental* longitudinal and transverse moments is described. Section 4 is devoted to a phenomenological analysis of the data at NLO, while the inclusion of the IR-renormalon uncertainties is presented in Section 5. The results of our final analysis of the transverse

data are collected in Section 6, and our main conclusions are summarised in Section 7.

2 The Operator Product Expansion and the Leading Twist

The complete Q^2 evolution of the structure functions can be obtained using the OPE [20] of the time-ordered product of the two currents entering the virtual-photon nucleon forward Compton scattering amplitude, viz.

$$T[J(z)\ J(0)] = \sum_{n,\alpha}\ f_n^\alpha(-z^2)\ z^{\mu_1} z^{\mu_2} ... z^{\mu_n}\ O^\alpha_{\mu_1\mu_2...\mu_n} \tag{1}$$

where $O^\alpha_{\mu_1\mu_2...\mu_n}$ are symmetric traceless operators of dimension d_n^α and twist $\tau_n^\alpha \equiv d_n^\alpha - n$, with α labelling different operators of spin n. In Eq. (1) $f_n^\alpha(-z^2)$ are coefficient functions, which are calculable in $pQCD$ at short-distance. Since the imaginary part of the forward Compton scattering amplitude is simply the hadronic tensor containing the structure functions measured in deep inelastic scattering (DIS) experiments, Eq. (1) leads to the well-known twist expansion for the Cornwall-Norton (CN) moments of the transverse structure function, viz.

$$\tilde{M}_n^T(Q^2) \equiv \int dx_0^1\ x^{n-2}\ F_2^N(x,Q^2) = \sum_{\tau=2,even}^{\infty} E_{n\tau}(\mu, Q^2)\ O_{n\tau}(\mu)\ \left(\frac{\mu^2}{Q^2}\right)^{\frac{\tau-2}{2}} \tag{2}$$

where μ is the renormalization scale, $O_{n\tau}(\mu)$ are the (reduced) matrix elements of operators with definite spin n and twist τ, containing the information about the non-perturbative structure of the target, and $E_{n\tau}(\mu, Q^2)$ are dimensionless coefficient functions, which can be expressed perturbatively as a power series of the running coupling constant $\alpha_s(Q^2)$.

As it is well known, in case of the leading twist ($\tau = 2$) one ends up with a non-singlet quark operator $\hat{O}^{NS}_{\tau=2}$ with corresponding matrix elements $O^{NS}_{n2} \equiv a_n^{NS}$ and coefficients E^{NS}_{n2}, and with singlet quark $\hat{O}^{S}_{\tau=2}$ and gluon $\hat{O}^{G}_{\tau=2}$ operators with corresponding matrix elements $a_n^\pm$ and coefficients $E^\pm_{n2}$ (after their mixing under renormalization group equations); explicitly one has

$$\tilde{M}_n^T(Q^2) = \mu_n^T(Q^2) + \text{higher twists} \tag{3}$$

$$\mu_n^T(Q^2) \equiv \mu_n^{NS}(Q^2) + \mu_n^S(Q^2) \tag{4}$$

with at NLO

$$\mu_n^{NS}(Q^2) = a_n^{NS}\ \left[\frac{\alpha_s(Q^2)}{\alpha_s(\mu^2)}\right]^{\gamma_n^{NS}}\ \frac{1+\alpha_s(Q^2)R_n^{NS}/4\pi}{1+\alpha_s(\mu^2)R_n^{NS}/4\pi} \tag{5}$$

$$\mu_n^{S}(Q^2) = a_n^{-}\ \left[\frac{\alpha_s(Q^2)}{\alpha_s(\mu^2)}\right]^{\gamma_n^{-}}\ \frac{1+\alpha_s(Q^2)R_n^{-}/4\pi}{1+\alpha_s(\mu^2)R_n^{-}/4\pi}\ + \ a_n^{+}\ \left[\frac{\alpha_s(Q^2)}{\alpha_s(\mu^2)}\right]^{\gamma_n^{+}}\ \frac{1+\alpha_s(Q^2)R_n^{+}/4\pi}{1+\alpha_s(\mu^2)R_n^{+}/4\pi} \tag{6}$$

where all the anomalous dimensions γ_n^i ($i = NS, \pm$) and coefficients R_n^i can be found in, e.g., Ref. [21] for $n \leq 10$ and for a number of active flavours, N_f, equal to $N_f = 3, 4$ and 5. At NLO the running coupling constant $\alpha_s(Q^2)$ is given by

$$\alpha_s(Q^2) = \frac{4\pi}{\beta_0 \ln(Q^2/\Lambda^2_{\overline{MS}})} \left\{ 1 - \frac{\beta_1}{\beta_0^2} \frac{\ln \ln(Q^2/\Lambda^2_{\overline{MS}})}{\ln(Q^2/\Lambda^2_{\overline{MS}})} \right\} \tag{7}$$

where $\Lambda_{\overline{MS}}$ is the QCD scale in the $\overline{MS}$ scheme, $\beta_0 = 11 - 2N_f/3$ and $\beta_1 = 102 - 38N_f/3$. The coefficients $a_n^{\pm}$ can be rewritten as follows

$$\begin{aligned} a_n^+ &= (1 - b_n)\ \mu_n^S(\mu^2)\ +\ c_n\ \mu_n^G(\mu^2) \\ a_n^- &= b_n\ \mu_n^S(\mu^2)\ -\ c_n\ \mu_n^G(\mu^2) \end{aligned} \tag{8}$$

where $\mu_n^G(Q^2)$ is the CN moment of the gluon distribution function $G(x, Q^2)$ of order n, viz. $\mu_n^G(Q^2) = \int_0^1 dx\ x^{n-2}\ G(x, Q^2)$. It turns out that, since quark and gluons are decoupled at large x, one has $b_n \sim 1$ and $c_n \sim 0$ already for $n \gtrsim 4$, so that only a_n^- contributes to Eq. (6). Moreover, again for $n \gtrsim 4$ one has $\gamma_n^- \simeq \gamma_n^{NS}$ and $R_n^-(f) \simeq R_n^{NS}$ [21], which implies that for $n \gtrsim 4$ the evolution of the leading-twist singlet moments $\mu_n^S(Q^2)$ almost coincide with that of the non-singlet ones $\mu_n^{NS}(Q^2)$. Therefore, when $n \geq 4$, we will consider for the leading twist term the following NLO expression

$$\mu_n^T(Q^2) = \mu_n^{NS}(Q^2) + \mu_n^S(Q^2) \rightarrow_{n \geq 4} a_n^{(2)}\ \left[\frac{\alpha_s(Q^2)}{\alpha_s(\mu^2)} \right]^{\gamma_n^{NS}}\ \frac{1 + \alpha_s(Q^2) R_n^{NS}/4\pi}{1 + \alpha_s(\mu^2) R_n^{NS}/4\pi} \tag{9}$$

with $a_n^{(2)} \equiv \mu_n^{NS}(\mu^2) + \mu_n^S(\mu^2)$. To sum up, the Q^2 evolution of the leading-twist transverse moments is completely determined by $pQCD$ for each spin n and all the unknown twist-2 parameters reduce to the three matrix elements a_2^{NS} and $a_2^{\pm}$ in case of the second moment, and only to one matrix element, $a_n^{(2)}$, for $n \geq 4$.

The contribution of power-like corrections to the Q^2 dependence of the moments (2) is due to higher twists corresponding to $\tau \geq 4$. Already at $\tau = 4$ the set of basic operators is quite large and their number grows rapidly as τ increases; moreover, each set of operators mix under renormalization group equations. The short-distance coefficients $E_{n\tau}$ can in principle be determined perturbatively, but the calculations are cumbersome and the large number of the involved matrix elements $O_{n\tau}(\mu)$ makes the resulting expression for the moments of limited use. Therefore, following Ref. [13], in this work we will make use of *effective* anomalous dimensions for the higher-twist terms (see next Section).

The OPE can be applied also to the longitudinal structure function $F_L^N(x, Q^2)$, where power corrections are expected to be more important than in the transverse case, because $F_L^N(x, Q^2)$ is vanishing at LO. However, NLO effects generate a non-vanishing contribution; more precisely, since the longitudinal structure function is defined as

$$F_L^N(x, Q^2) \equiv F_2^N(x, Q^2)\ \left(1 + \frac{4M^2x^2}{Q^2} \right)\ \frac{R_{L/T}^N(x, Q^2)}{1 + R_{L/T}^N(x, Q^2)} \tag{10}$$

where $R^N_{L/T}(x,Q^2) \equiv \sigma^N_L(x,Q^2)/\sigma^N_T(x,Q^2)$ is the L/T cross section ratio, one has

$$\tilde{M}^L_n(Q^2) \equiv \int_0^1 dx\ x^{n-2}\ F^N_L(x,Q^2) = \mu^L_n(Q^2) + \text{higher twists} \tag{11}$$

with the leading-twist contribution $\mu^L_n(Q^2)$ given at NLO by

$$\mu^L_n(Q^2) = \frac{\alpha_s(Q^2)}{4\pi}\frac{1}{n+1}\left\{\frac{8}{3}\mu^q_n(Q^2) + \frac{2d}{n+2}\mu^G_n(Q^2)\right\} + \mu^c_n(Q^2) \tag{12}$$

where $\mu^q_n(Q^2)$ is the light-quark flavour contribution to the n-th moment of the transverse structure function, $\mu^c_n(Q^2)$ is the charm quark contribution (starting when the invariant produced mass W is greater than twice the mass of the charm quark), and $d = 12/9$ and $20/9$ for $N_f = 3$ and 4, respectively. In what follows Eq. (12) will be evaluated using sets of parton distributions available in the literature (see Section 5).

For massless targets only operators with spin n contribute to the n-th CN moments of both the longitudinal and transverse structure functions. When the target mass is non-vanishing, operators with different spins can contribute and consequently the higher-twist terms in the expansion of the CN moments $\tilde{M}^T_n(Q^2)$ and $\tilde{M}^L_n(Q^2)$ contain now also target-mass terms, which are of pure kinematical origin. It has been shown by Natchmann [22] that even when $M \neq 0$ the moments can be redefined in such a way that only spin-n operators contribute in the n-th moment, namely

$$M^T_n(Q^2) \equiv \int_0^1 dx \frac{\xi^{n+1}}{x^3} F^N_2(x,Q^2)\frac{3+3(n+1)r+n(n+2)r^2}{(n+2)(n+3)} \tag{13}$$

$$M^L_n(Q^2) \equiv \int_0^1 dx \frac{\xi^{n+1}}{x^3}\left[F^N_L(x,Q^2) + \frac{4M^2x^2}{Q^2}F^N_2(x,Q^2)\frac{(n+1)\xi/x - 2(n+2)}{(n+2)(n+3)}\right] \tag{14}$$

where $r \equiv \sqrt{1+4M^2x^2/Q^2}$ and $\xi \equiv 2x/(1+r)$ is the Natchmann variable. Using the *experimental* $F^N_2(x,Q^2)$ and $F^N_L(x,Q^2)$ in the r.h.s. of Eqs. (13-14), the target-mass corrections are cancelled out and therefore the twist expansions of the experimental Natchmann moments $M^T_n(Q^2)$ and $M^L_n(Q^2)$ contain only *dynamical* twists, viz.

$$M^T_n(Q^2) = \mu^T_n(Q^2) + \text{dynamical higher twists} \tag{15}$$

$$M^L_n(Q^2) = \mu^L_n(Q^2) + \text{dynamical higher twists} \tag{16}$$

where the leading-twist terms $\mu^T_n(Q^2)$ and $\mu^L_n(Q^2)$ are given at NLO by Eqs. (4-6) and (12), respectively.

3 Data on Transverse and Longitudinal Moments

For the evaluation of the Natchmann transverse $M^T_n(Q^2)$ (Eq. (13)) as well as longitudinal $M^L_n(Q^2)$ (Eq. (14)) moments systematic measurements of the experimental structure functions $F^N_2(x,Q^2)$ and $F^N_L(x,Q^2)$ are required in the whole x-range at fixed values of Q^2.

However, such measurements are not always available and therefore we have adopted interpolation formulae ("pseudo-data"), which fit the considerable amount of existing data on the proton and deuteron structure functions.

In case of the transverse channel we have used: i) the Bodek's fit [2, 7] to the inclusive (e, e') $SLAC$ data in the resonance region for values of the invariant produced mass W smaller than 2.5 GeV, and ii) the Tulay's fit [8] to the world data in the DIS region for $W > 2.5$ GeV. In order to have continuity at $W = 2.5$ GeV the Bodek's fit has been divided by a factor 1.03 (at any Q^2), which is inside the experimental errors. Moreover, we have also taken into account the wealth of $SLAC$ proton data [3] beyond $x \simeq 0.7$ up to $x \simeq 0.98$ through a simple interpolation fit given in Ref. [3]. All these fits cover the range of x which is crucial for the evaluation of the moments considered in this work; therefore, the uncertainties on the moments are related only to the accuracy of the interpolation formulae; the latter are simply given by a $\pm 4\%$ total (systematic + statistical) error reported for the $SLAC$ data [2, 3] and by the upper and lower bounds of the Tulay's fit quoted explicitly in Ref. [8]. Finally, since the whole set of DIS (unpolarised) $SLAC$ and $BCDMS$ data (on which also the Tulay's fit is based) is known to favour the value $\alpha_s(M_Z^2) \simeq 0.113$ (see Ref. [12]), in what follows the value $\Lambda_{\overline{MS}} = 290$ (240) MeV at $N_f = 3$ (4) will be adopted for the calculation of the running coupling constant at NLO via Eq. (7)[b].

As for the longitudinal channel, the structure function $F_L^N(x, Q^2)$ is reconstructed via Eq. (10), using for the L/T ratio the phenomenological fit (and the interpolation uncertainties) provided in Ref. [11]. In the nucleon resonance region the ratio $R_{L/T}^N(x, Q^2)$ has been taken from Ref. [24] for the lowest values of Q^2 (namely $Q^2 = 1 \div 2$ $(GeV/c)^2$), while it has been assumed to be equal to zero for $Q^2 > 2$ $(GeV/c)^2$, which is consistent with the limited amount of available data [25].

Since the OPE is totally inclusive, the contribution of the nucleon elastic channels has to be included in the calculation of the moments, viz.

$$\begin{aligned} F_2^N(x, Q^2) &= F_2^{N(inel)}(x, Q^2) + F_2^{N(el)}(x, Q^2) \\ F_L^N(x, Q^2) &= F_L^{N(inel)}(x, Q^2) + F_L^{N(el)}(x, Q^2) \end{aligned} \tag{17}$$

and consequently

$$\begin{aligned} M_n^T(Q^2) &= \left[M_n^T(Q^2)\right]_{inel} + \left[M_n^T(Q^2)\right]_{el} \\ M_n^L(Q^2) &= \left[M_n^L(Q^2)\right]_{inel} + \left[M_n^L(Q^2)\right]_{el} \end{aligned} \tag{18}$$

In case of the proton one has

$$F_2^{p(el)}(x, Q^2) = \delta(x-1)\, \frac{[G_E^p(Q^2)]^2 + \eta\, [G_M^p(Q^2)]^2}{1+\eta} \tag{19}$$

$$F_L^{p(el)}(x, Q^2) = \delta(x-1)\, \frac{[G_E^p(Q^2)]^2}{\eta} \tag{20}$$

[b] The impact of a different value of $\alpha_s(M_Z^2)$, much closer to the updated PDG value $\alpha_s(M_Z^2) = 0.119 \pm 0.002$ [23], will be briefly addressed at the end of Section 5.

where $G_E^p(Q^2)$ and $G_M^p(Q^2)$ are the electric and magnetic (Sachs) proton form factors, respectively, and $\eta \equiv Q^2/4M^2$. Thus, the contribution of the proton elastic channel is explicitly given by

$$\begin{aligned}\left[M_n^T(Q^2)\right]_{el} \;\rightarrow_{proton}\; & \left(\frac{2}{1+r^*}\right)^{n+1} \frac{3+3(n+1)r^*+n(n+2)r^{*2}}{(n+2)(n+3)} \\ & \frac{[G_E^p(Q^2)]^2+\eta\,[G_M^p(Q^2)]^2}{1+\eta} \qquad (21)\end{aligned}$$

$$\begin{aligned}\left[M_n^L(Q^2)\right]_{el} \;\rightarrow_{proton}\; & \frac{1}{1+\eta}\left(\frac{2}{1+r^*}\right)^{n+1}\Big\{[G_E^p(Q^2)]^2-[G_M^p(Q^2)]^2+ \\ & \frac{n+1}{n+3}\left[1+\frac{2}{(n+2)(1+r^*)}\right]\frac{[G_E^p(Q^2)]^2+\eta\,[G_M^p(Q^2)]^2}{1+\eta}\Big\} \qquad (22)\end{aligned}$$

with $r^* = \sqrt{1+4M^2/Q^2} = \sqrt{1+1/\eta}$.

In case of the deuteron the folding of the nucleon elastic channel with the momentum distribution of the nucleon in the deuteron gives rise to the so-called quasi-elastic peak. In the Q^2-range of interest the existing data are only fragmentary and therefore we have computed $F_2^{D(el)}(x,Q^2)$ and $F_L^{D(el)}(x,Q^2)$ using the procedure of Ref. [26], which includes the folding of the nucleon elastic peak with the nucleon momentum distribution in the deuteron as well as final state interaction effects; such procedure can be applied both at low ($Q^2 \lesssim 1\ (GeV/c)^2$) and high values of Q^2 (see Ref. [27]). The results of the calculations, performed using the deuteron wave function corresponding to the Paris nucleon-nucleon potential [28], are compared in Fig. 1 with the *SLAC* data of Ref. [29] at $Q^2 = 1.75$ and $3.25\ (GeV/c)^2$. It can be seen that the agreement with the data is quite good for the transverse part and still acceptable for the less accurate longitudinal response.

In Figs. 2 and 3 the Q^2 behaviours of the inelastic, elastic and total transverse moments are reported for the proton and the deuteron, respectively, in the whole Q^2-range of interest in this work, i.e. $1 \lesssim Q^2(GeV/c)^2 \lesssim 20$. Note that in case of the deuteron our data refer to the moments of the structure function per nucleon. It can clearly be seen that the inelastic and elastic contributions exhibit quite different Q^2-behaviours and, in particular, the inelastic part turns out to be dominant for $Q^2 \gtrsim 1\ (GeV/c)^2$ in the second moment and only for $Q^2 \gtrsim n\ (GeV/c)^2$ in higher order moments. The Q^2-behaviour of the longitudinal moments is illustrated in Figs. 4 an 5 in case of the proton and the deuteron, respectively. It can be seen that the elastic contribution drops quite fast and it is relevant only at the lowest values of Q^2 ($Q^2 \simeq$ few $(GeV/c)^2$).

We point out that our present determination of the longitudinal and transverse *experimental* moments is clearly limited by the use of phenomenological fits of existing data (i.e. *"pseudo-data"*), which are required in order to interpolate the structure functions in the whole x-range for fixed values of Q^2, as well as by the existing large uncertainties in the determination of the L/T ratio $R_{L/T}^N(x,Q^2)$. Thus, both transverse data with better quality at $x \gtrsim 0.6$ and $Q^2 \lesssim 10\ (GeV/c)^2$ and more precise, systematic determinations of the L/T cross section ratio are still required to improve our experimental knowledge of the Q^2-behaviour of the low-order moments of the nucleon structure functions.

4 Analysis of the Transverse Data at NLO

In this Section we present our analysis of the transverse *pseudo-data* of Figs. 2 and 3, adopting for the leading twist the NLO expressions (5-6) and for the power corrections a purely phenomenological ansätz. Indeed, as already pointed out, several higher-twist operators exist and mix under the renormalization-group equations; such a mixing is rather involved (see, e.g., Ref. [30] in case of twist-4 operators) and in particular the number of mixing operators increases with the spin n. Since complete calculations of the higher-twist anomalous dimensions are not yet available, we use the phenomenological ansätz already adopted in Ref. [13], which in case of the second moment $M^T_{n=2}(Q^2)$ leads to the expansion

$$M_2^T(Q^2) = \mu_2^{NS}(Q^2) + \mu_2^S(Q^2) + a_2^{(4)} \left[\frac{\alpha_s(Q^2)}{\alpha_s(\mu^2)}\right]^{\gamma_2^{(4)}} \frac{\mu^2}{Q^2} \tag{23}$$

where the logarithmic $pQCD$ evolution of the twist-4 contribution is accounted for by the term $[\alpha_s(Q^2)/\alpha_s(\mu^2)]^{\gamma_2^{(4)}}$ with an *effective* anomalous dimension $\gamma_2^{(4)}$ and the parameter a_2^4 represents the overall strength of the twist-4 term at $Q^2 = \mu^2$. For the QCD renormalization scale μ we adopt hereafter the value $\mu = 1\ GeV/c$. We have explicitly checked that a different choice for μ does not modify any conclusion of this work, because (e.g. in Eq. (23)) the values of the parameter a_2^4 corresponding to two different choices μ and μ' turn out to be related by the logarithmic $pQCD$ evolution, i.e. $a_2^4(\mu') = a_2^4(\mu)\ [\alpha_s(\mu'^2)/\alpha_s(\mu^2)]^{\gamma_2^4}\ \mu^2/\mu'^2$.

The unknown parameters appearing in Eq. (23) (i.e., the three twist-2 parameters $a_2^{NS} \equiv \mu_2^{NS}(Q^2 = \mu^2)$, $a_2^S \equiv \mu_2^S(Q^2 = \mu^2)$ and $a_2^G \equiv \mu_2^G(Q^2 = \mu^2)$ and the two twist-4 parameters $a_2^{(4)}$ and $\gamma_2^{(4)}$) have been determined by fitting our data for the proton and the deuteron (see Fig. 2(a) and 3(a), respectively), adopting the least-χ^2 procedure in the Q^2-range between 1 and 20 $(GeV/c)^2$. It turned out that the singlet and gluon twist-2 parameters can be directly determined form the data only in case of the deuteron, but not in case of the proton. Thus, in fitting the proton data we have kept fixed the parameters a_2^S and a_2^G at the values obtained for the deuteron. Our results are shown in Figs. 6(a) and 7(a) in the whole Q^2-range of the analysis, while the values obtained for the various parameters are reported in Table 1, together with the uncertainties of the fitting procedure corresponding to one-unit increment of the χ^2/N variable (where N is the number of degrees of freedom). It can clearly be seen that:

- the twist-4 contribution to second transverse moment $M_2^T(Q^2)$ is quite small in the proton and is almost vanishing in the deuteron in the whole Q^2-range of our analysis; the latter result suggests that the twist-4 effect in the neutron comes with a sign opposite to that in the proton at variance with the expectations from the bag model [31];

- the twist-4 contribution in the proton at $Q^2 = \mu^2 = 1\ (GeV/c)^2$ (i.e., $a_2^{(4)} = 0.012 \pm 0.010$) turns out to be significantly smaller than the result $a_2^{(4)} = 0.030 \pm 0.003$ quoted in Ref. [13], where however the twist-2 term was not simultaneously fitted to the data, but instead it was calculated using the parton densities of Ref. [32] evolved at

NLO. Therefore, we have repeated our analysis by fixing the twist-2 term at the *GRV* prediction [32] obtaining $a_2^{(4)} = 0.02 \pm 0.01$, which is still lower but not inconsistent within the errors with the result of Ref. [13]. We point out that a small variation of the twist-2 term can affect significantly the strength of the small twist-4 term; that is why our uncertainty from a simultaneous a_2^{NS} and $a_2^{(4)}$ fit appears to be quite larger than the one found in Ref. [13];

- as a cross-check, we have also fitted separately the non-singlet parameter a_2^{NS} to the "$(p-n)/2$" data, defined as the difference between the proton and deuteron data, obtaining $a_2^{NS} = 0.029 \pm 0.009$, $a_2^{(4)} = 0.012 \pm 0.010$ and $\gamma_2^{(4)} = 1 \pm 1$. Combining these results with those found in the deuteron, we expect to get in case of the proton $a_2^{NS} = 0.096 \pm 0.017$, $a_2^{(4)} = 0.012 \pm 0.010$ and $\gamma_2^{(4)} = 1 \pm 1$, which indeed are in nice agreement with the proton fit results of Table 1.

As described in Section 2, in case of the transverse moments $M_n^T(Q^2)$ with $n \geq 4$ the evolution of the twist-2 contribution can be simplified and assumed to be a pure non-singlet one; therefore, we have considered the following twist expansion

$$M_{n\geq 4}^T(Q^2) = \mu_n^T(Q^2) + a_n^{(4)} \left[\frac{\alpha_s(Q^2)}{\alpha_s(\mu^2)}\right]^{\gamma_n^{(4)}} \frac{\mu^2}{Q^2} + a_n^{(6)} \left[\frac{\alpha_s(Q^2)}{\alpha_s(\mu^2)}\right]^{\gamma_n^{(6)}} \frac{\mu^4}{Q^4} \qquad (24)$$

where the leading twist term $\mu_n^T(Q^2)$ is given at *NLO* by Eq. (9) and $\mu = 1$ *GeV/c*. All the five unknown parameters (i.e., $a_n^{(2)}$, $a_n^{(4)}$, $\gamma_n^{(4)}$, $a_n^{(6)}$ and $\gamma_n^{(6)}$) have been determined from the data through the least-χ^2 procedure for each value of n. The results are shown in Figs. 6 and 7, while the values of the parameters are reported in Tables 2 and 3 in case of the proton and deuteron, respectively. Our main results can be summarised as follows:

- our twist-2 term, extracted from the proton data together with the twist-4 and twist-6 contributions, differs only slightly from the predictions obtained using the set of parton distributions of Ref. [32] evolved at *NLO* (see dashed lines in Fig. 6). We have checked that, by repeating our analysis with the twist-2 term fixed at the *GRV* prediction, the values of all the higher-twist parameters appearing in Eq. (24) change for $n > 2$ only within the errors reported in Tables 2 and 3;

- the twist-4 and twist-6 contributions result to have opposite signs and, moreover, at $Q^2 \sim 1$ $(GeV/c)^2$ they are approximately of the same order of magnitude. The negative sign of the twist-6 is clearly due to the fact that a fit with a twist-4 term alone overestimates the low Q^2 data ($Q^2 \simeq$ few $(GeV/c)^2$). We stress that the opposite signs found for the twist-4 and twist-6 terms make the total higher-twist contribution smaller than its individual terms; in particular, at large Q^2 the sum of the twist-4 and twist-6 contributions turns out to be a small fraction of the twist-2 term ($\lesssim 10\%$ for $Q^2 \gtrsim n$ $(GeV/c)^2$).

- the values of the effective anomalous dimensions $\gamma_n^{(4)}$ and $\gamma_n^{(6)}$ for $n = 4, 6, 8$ result to be around 4.0 and 2.5, respectively, i.e. significantly larger than the values of the corresponding twist-2 anomalous dimensions ($\gamma_n^{NS} \simeq 0.8 \div 1.2$ for $n = 4, 6, 8$ [21]);

- the uncertainties on the different twist contributions due to the parameter fitting procedure are always within $\pm 15\%$ (see Fig. 7 in case of the deuteron);
- the twist expansions (23) and (24) appear to work quite well for values of Q^2 down to $\simeq 1\ (GeV/c)^2$.

An interesting feature of our analysis of the transverse moments is that the leading-twist contribution is extracted from the analysis and not fixed by calculations based on a particular set of parton distributions. The comparison of our extracted twist-2 term with the predictions based on the GRV parton distributions [32] is shown in Fig. 8 for $Q^2 \gtrsim 5\ (GeV/c)^2$. It can clearly be seen that our results and the GRV predictions agree quite well in case of the proton, whereas they differ significantly in case of the deuteron for $n > 2$. The inclusion of a new empirical determination of the nuclear effects in the deuteron, obtained in Ref. [33] from the nuclear dependence of the $SLAC$ data, increases only a little bit the disagreement for $n > 2$ (see dashed lines in Fig. 8). Since moments with $n > 2$ are mostly sensitive to the high-x behaviour of the structure function, the question arises whether our extracted twist-2 moments can be explained by an enhancement of the d-quark parton distribution, like the one advocated in Ref. [16], which explicitly reads as $\tilde{d}(x) = d(x) + 0.1x(1+x)u(x)$. The *modified GRV* predictions, including also the empirical nuclear corrections for the deuteron, are shown by the solid lines in Fig. 8 and agree quite well with our results both for the proton and the deuteron. Therefore, our extracted twist-2 moments are clearly compatible with the hypothesis of an enhancement of the d-quark distribution at large x.

So far the power corrections appearing in Eqs. (23-24) have been derived assuming for the leading twist the NLO in the strong coupling constant. Since our main aim is to try to estimate the target-dependent power corrections generated by multiparton correlations, it is necessary to estimate the possible effects of higher orders of the perturbative series, which defines the twist-2 coefficient functions $E_{n2}(\mu, Q^2)$ appearing in Eq. (2). However, it is well known that such series is asymptotic at best and affected by the so-called IR-renormalon ambiguities [34]. More precisely, the only way to interpret consistently the large order behaviour of the pertubartion theory leads unavoidably to ambiguities which have the general form of power-suppressed terms. This happens because certain classes of high-order radiative corrections to the twist-2 (the so-called fermion bubble chains) are sensitive to large distances (i.e., to the non-perturbative domain). Nevertheless it should be stressed that the IR-renormalon contribution to the twist-2 has to cancel against the ultraviolet quadratic divergencies of twist-4 operators (see, e.g., Refs. [34, 35, 15]). This means that each twist in the expansion (2) is not defined unambigously, while the entire sum (i.e., the complete calculation) is free from ambiguities. Therefore, while the data cannot be affected by IR-renormalon uncertainties, our fitting procedure, based on the separation among various twists and on the theoretical perturbative treatment of the leading twist only, can suffer from IR-renormalon ambiguities. The latter are target-independent quantities, being of pure perturbative nature, while genuine higher-twist effects are related to multiparton correlations in the target (i.e., target-dependent quantities).

The IR-renormalon picture has been applied to the phenomenology of deep inelastic

lepton-hadron scattering as a guide to estimate the x dependence of power corrections [14, 15]. Such an estimate has been found to be a good guess in case of the proton and the deuteron structure functions and this fact may be understandable in terms of the notion of a universal IR-finite effective strong coupling constant [36] or in terms of the hypothesis of the dominance of the quadratically divergent parts of the matrix elements of twist-4 operators [37].

Before closing this Section, we point out that the IR-renormalon contribution behaves as a power-like term, but it is characterised by twist-2 anomalous dimensions. Thus, our observation that for $n = 4, 6, 8$ the effective anomalous dimensions $\gamma_n^{(4)}$ and $\gamma_n^{(6)}$ extracted from our NLO fit to the transverse data are significantly different from the corresponding twist-2 anomalous dimensions, might be an indication of the presence of multiparton correlation effects (at least) in the transverse channel. In order to try to disentangle the latter from large order perturbative effects, we will consider explicitly in the next Section the power-like terms associated to the IR renormalons as the general uncertainty in the perturbative prediction of the twist-2 [38].

5 IR Renormalons and the Analysis of the Longitudinal Channel

Within the naive non-abelianization (NNA) approximation the contribution of the renormalon chains (i.e. the sum of vacuum polarisation insertions on the gluon line at one-loop level) to the non-singlet parts of the nucleon structure functions $F_1^N(x,Q^2)$ and $F_2^N(x,Q^2)$ is given by [14]

$$F_1^{IR}(x,Q^2) = \int_x^1 dz\ F_1^{LT}(\frac{x}{z},Q^2)\ \left[A_2^{IR}\frac{D_2(z)}{Q^2} + A_4^{IR}\frac{D_4(z)}{Q^4}\right] \tag{25}$$

$$F_2^{IR}(x,Q^2) = \int_x^1 dz\ F_2^{LT}(\frac{x}{z},Q^2)\ \left[A_2^{IR}\frac{C_2(z)}{Q^2} + A_4^{IR}\frac{C_4(z)}{Q^4}\right] \tag{26}$$

where the constants A_2^{IR} and A_4^{IR} are related to the log-moments of an IR-finite effective strong coupling constant [36], F_1^{LT} and F_2^{LT} are the leading-twist structure functions and the coefficient functions $C_{2(4)}$ and $D_{2(4)}$ are given explicitly in Ref. [14]. Thus, the IR-renormalon contribution to the transverse and longitudinal moments is explicitly given by

$$\mu_n^{T(IR)}(Q^2) = \mu_n^{NS}(Q^2)\left\{\frac{A_2^{IR}}{Q^2}\tilde{C}_2(n) + \frac{A_4^{IR}}{Q^4}\tilde{C}_4(n)\right\} \tag{27}$$

$$\mu_n^{L(IR)}(Q^2) = \mu_n^{NS}(Q^2)\left\{\frac{A_2^{IR}}{Q^2}\left[\frac{8\alpha_s(Q^2)}{6\pi}\frac{\tilde{D}_2(n)}{n+1} - \frac{4n}{n+2}\right] + \frac{A_4^{IR}}{Q^4}\left[\frac{8\alpha_s(Q^2)}{6\pi}\frac{\tilde{D}_4(n)}{n+1} - 4n\frac{n+1}{n+3}\right]\right\} \tag{28}$$

where in the last equation we have used the non-singlet part of the NLO relation (12). The coefficients $\tilde{C}_{2(4)}(n)$ and $\tilde{D}_{2(4)}(n)$ read as follows [14]

$$\tilde{C}_2(n) = -n - 8 + \frac{4}{n} + \frac{2}{n+1} + \frac{12}{n+2} + 4S_n \tag{29}$$

$$\tilde{C}_4(n) = \frac{1}{2}n^2 - \frac{3}{2}n + 16 - \frac{4}{n} - \frac{4}{n+1} - \frac{36}{n+3} - 4S_n$$

$$\tilde{D}_2(n) = -n - 4 + \frac{4}{n} + \frac{2}{n+1} + \frac{4}{n+2} + 4S_n \tag{30}$$

$$\tilde{D}_4(n) = \frac{1}{2}n^2 + \frac{5}{2}n + 8 - \frac{4}{n} - \frac{4}{n+1} - \frac{12}{n+3} - 4S_n \tag{31}$$

where $S_n \equiv \sum_{j=1}^{n-1}(1/j)$. As already mentioned, Eqs. (27-28) describe the contributions of IR renormalons to the non-singlet structure functions, while the more involved case of the singlet parts of the DIS structure functions has been recently investigated in Ref. [39]. There it has been shown that the difference between the IR-renormalon contributions to the singlet and non-singlet moments is not relevant for $n \geq 4$ thanks to the quark-gluon decoupling at large x. Therefore, for $n \geq 4$ it suffices to consider Eqs. (27-28) after substituting $\mu_n^{NS}(Q^2)$ with $\mu_n^T(Q^2)$, given at NLO by Eq. (9).

An interesting feature of the IR-renormalon terms (27-28) is that they are mainly governed by the values of only two (unknown) parameters, A_2^{IR} and A_4^{IR}, which appear simultaneously both in the longitudinal and transverse channels at any value of n. The signs of A_2^{IR} and A_4^{IR} are not theoretically known, because they depend upon the prescription used to circumvent the renormalon singularities of the Borel integrals, while within the NNA approximation their absolute values may be provided by [15]

$$|A_2^{IR}| = \frac{6C_F\Lambda^2_{\overline{MS}}}{33-2N_f}e^{5/3} \quad , \qquad |A_4^{IR}| = \frac{3C_F\Lambda^4_{\overline{MS}}}{33-2N_f}e^{10/3} \tag{32}$$

with $C_F = 4/3$. Using for $\Lambda_{\overline{MS}}$ the same values adopted for the NLO calculation of $\alpha_s(Q^2)$ (see previous Section), one gets that $|A_2^{IR}|$ varies from 0.10 to 0.13 GeV^2, while $|A_4^{IR}|$ ranges from 0.015 to 0.030 GeV^4 for $N_f = 3, 4$.

First of all, we have checked whether the power corrections to the NLO twist-2 contribution in the transverse channel can be explained by pure IR-renormalon terms in the whole range $1 \lesssim Q^2\ (GeV/c)^2 \lesssim 20$. It turns out that: i) the quality of the resulting fit is not as good as the one obtained via the expansion (24) and the obtained minima of the χ^2/N variable can be much larger than 1; ii) the extracted values of $|A_2^{IR}|$ and $|A_4^{IR}|$ result to be much greater than the NNA expectations (32) and to depend strongly upon the inclusion of the data at low Q^2 ($Q^2 \sim$ few $(GeV/c)^2$). Moreover, the IR-renormalon contribution to the longitudinal moments (Eq. (28)), calculated using the values of A_2^{IR} and A_4^{IR} determined from the analysis of the transverse channel, leads to a large overestimation of the longitudinal data, as already noted in Ref. [15]. These results may be viewed as an effect of the presence of higher-twist terms generated by multiparton correlations in the transverse data for $Q^2 \gtrsim 1\ (GeV/c)^2$. To make this statement more quantitative, we start with the

analysis of the longitudinal data adopting for the power corrections a pure IR-renormalon picture; namely, for $n \geq 4$ we have used the following expansion

$$M_n^L(Q^2) \;=\; \mu_n^L(Q^2) + \mu_n^{L(IR)}(Q^2) \;\to_{n\geq 4}\; \mu_n^L(Q^2) + \mu_n^T(Q^2) \cdot \left\{ \frac{A_2^{IR}}{Q^2} \left[\frac{8\alpha_s(Q^2)}{6\pi} \frac{\tilde{D}_2(n)}{n+1} - \frac{4n}{n+2} \right] + \frac{A_4^{IR}}{Q^4} \left[\frac{8\alpha_s(Q^2)}{6\pi} \frac{\tilde{D}_4(n)}{n+1} - 4n \frac{n+1}{n+3} \right] \right\} \quad (33)$$

where $\mu_n^L(Q^2)$ is given by Eq. (12) and calculated using the GRV parton distributions [32], while $\mu_n^T(Q^2)$ (see Eq. (9)) is taken from the NLO analysis of the transverse data made in the previous Section (see Tables 2 and 3 for the values of the twist-2 parameters $a_n^{(2)}$).

For each value of $n \geq 4$ we have determined the values of A_2^{IR} and A_4^{IR} from the least-χ^2 fit to the longitudinal data in the whole range $1 \lesssim Q^2\ (GeV/c)^2 \lesssim 20$; our results are reported in Tables 4-5 and Figs. 9-10 in case of proton and deuteron targets, respectively. It can clearly be seen that: i) the extracted values of A_2^{IR} are almost independent of n, which means that the n-dependence (i.e., the shape in x) of the $1/Q^2$ power correction is nicely predicted by the NNA approximation; ii) the values obtained for $|A_2^{IR}|$ are only slightly larger than the NNA expectation (32); iii) the determination of A_4^{IR} is almost compatible with zero and affected by large uncertainties, since the $1/Q^4$ power corrections turn out to be quite small in the longitudinal channel; nevertheless; the extracted values are not completely inconsistent with the NNA predictions (32); iv) the power corrections appear to be approximately the same in the proton and deuteron longitudinal channels (as it can be expected from a pure IR-renormalon phenomenology).

As for the second moment $M_2^L(Q^2)$ we have simplified our analysis by taking only the non-singlet IR-renormalon contribution (28), i.e. by totally neglecting its singlet part. This is an approximation, but the resulting fit to the data on $M_2^L(Q^2)$ turns out to be quite good as it can be seen from Figs. 9(a) and 10(a), yielding values of A_2^{IR} and A_4^{IR} only slightly different from the ones previously determined by the analysis of the moments with $n \geq 4$ (see Tables 4 and 5).

To sum up, in case of both proton and deuteron targets a pure IR-renormalon description of power corrections works quite nicely in the longitudinal channel starting already at $Q^2 \simeq 1\ (GeV/c)^2$. Averaging the results of Tables 4 and 5 for $n \geq 4$ only, our determination of the IR-renormalon strength parameters results to be: $A_2^{IR} \simeq -0.132 \pm 0.015\ GeV^2$ and $A_4^{IR} \simeq 0.009 \pm 0.003\ GeV^4$, which, we stress, are not inconsistent with the NNA expectations (32). Moreover, the value found for A_2^{IR} nicely agrees with the corresponding findings of Ref. [17], recently obtained from a NLO analysis of the $CCFR$ data [18] on $xF_3^N(x, Q^2)$.

Before closing this section, we stress again that the IR-renormalon power-like terms should be regarded as the general uncertainty in the perturbative calculation of the twist-2 term. Thus, it is worth recalling that our estimates of the IR-renormalon parameters have been obtained by taking the perturbative calculation of the twist-2 term at NLO. We expect that our determination of the IR-renormalon parameters holds only at NLO and would vary if higher orders of the perturbation theory were included. As a matter of fact, a significative reduction of the IR-renormalon terms seems to be suggested by the recent $NNLO$ results quoted in Refs. [16] and [17].

6 Final Analysis of the Transverse Data

After having determined the strengths and signs of the twist-4 and twist-6 IR-renormalon contributions from the analysis of the longitudinal channel, we can now proceed to the final analysis of the transverse data, adopting the following twist expansion

$$M_n^T(Q^2) = \mu_n^T(Q^2) + \mu_n^{T(IR)}(Q^2) + a_n^{(4)} \left[\frac{\alpha_s(Q^2)}{\alpha_s(\mu^2)}\right]^{\gamma_n^{(4)}} \frac{\mu^2}{Q^2} + a_n^{(6)} \left[\frac{\alpha_s(Q^2)}{\alpha_s(\mu^2)}\right]^{\gamma_n^{(6)}} \frac{\mu^4}{Q^4} \quad (34)$$

where now the higher-twist terms involving the parameters $a_n^{(4)}$, $\gamma_n^{(4)}$, $a_n^{(6)}$ and $\gamma_n^{(6)}$ should be related to (target-dependent) multiparton correlation effects. Collecting Eqs. (9) and (27) one has for $n \geq 4$

$$\begin{aligned} M_{n\geq 4}^T(Q^2) &= a_n^{(2)} \left[\frac{\alpha_s(Q^2)}{\alpha_s(\mu^2)}\right]^{\gamma_n^{NS}} \frac{1+\alpha_s(Q^2)R_n^{NS}/4\pi}{1+\alpha_s(\mu^2)R_n^{NS}/4\pi} \left\{1 + \frac{A_2^{IR}}{Q^2}\tilde{C}_2(n) + \frac{A_4^{IR}}{Q^4}\tilde{C}_4(n)\right\} + \\ & a_n^{(4)} \left[\frac{\alpha_s(Q^2)}{\alpha_s(\mu^2)}\right]^{\gamma_n^{(4)}} \frac{\mu^2}{Q^2} + a_n^{(6)} \left[\frac{\alpha_s(Q^2)}{\alpha_s(\mu^2)}\right]^{\gamma_n^{(6)}} \frac{\mu^4}{Q^4} \end{aligned} \quad (35)$$

The IR-renormalon parameters A_2^{IR} and A_4^{IR} have been kept fixed at the values $A_2^{IR} = -0.132\ GeV^2$ and $A_4^{IR} = 0.009\ GeV^4$ found in the previous Section, while the values of the five parameters $a_n^{(2)}$, $a_n^{(4)}$, $\gamma_n^{(4)}$, $a_n^{(6)}$ and $\gamma_n^{(6)}$ have been determined through the least-χ^2 procedure and reported in Tables 6 and 7 in case of proton and deuteron, respectively. Comparing with the results obtained without the IR-renormalon contributions (see Tables 2 and 3), it can be clearly seen that the values of the twist-2 parameters $a_n^{(2)}$ are almost unchanged, while the values of the higher-twist parameters $a_n^{(4)}$, $\gamma_n^{(4)}$, $a_n^{(6)}$ and $\gamma_n^{(6)}$ vary only within the uncertainties of the fitting procedure. Note that with the inclusion of the IR-renormalon contribution the sum $a_n^{(4)} + a_n^{(6)}$ is closer to zero, which implies that at $Q^2 \simeq \mu^2 = 1\ (GeV/c)^2$ the twist-4 and twist-6 terms generated by multiparton correlation almost totally compensate each other. Such an effect is clearly illustrated in Figs. 11 and 12, where the contributions of the twist-2 at NLO, of the IR-renormalon and of the multiparton correlations are separately reported. From Figs. 11 and 12 it can be also seen that, for $n \geq 4$, the IR-renormalon contribution increases significantly around $Q^2 \sim 1\ (GeV/c)^2$ and could become of the same order of magnitude of the twist-2 term at NLO in case of higher order moments. The effects from multiparton correlations appear to exceed the IR-renormalon term only for $Q^2 \gtrsim 2\ (GeV/c)^2$ (at $n \geq 4$).

As for the second moment $M_2^T(Q^2)$, following our previous analyses, we apply the IR-renormalon correction only to the non-singlet twist-2 term; moreover, the twist-2 parameters a_2^S and a_2^G are kept fixed at the values given in Table 1 for the deuteron and only the twist-4 term $a_n^{(4)}\ [\alpha_s(Q^2)/\alpha_s(\mu^2)]^{\gamma_n^{(4)}}\ (\mu^2/Q^2)$ is explicitly considered in the analysis. The resulting value of the twist-2 parameter a_2^{NS} is 0.096 ± 0.006 (0.066 ± 0.0044) for the proton (deuteron), which coincides within the uncertainties with the one given in Table 1. The twist-4 parameter $a_2^{(4)}$ turns out to be almost compatible with zero, namely $a_2^{(4)} = 0.01 \pm 0.01$ for the proton and $|a_2^{(4)}| \lesssim 10^{-3}$ for the deuteron. Considering also the results of the previous Section on

the longitudinal channel, our analyses indicate that the smallness of multiparton correlation effects on the second moments (both transverse and longitudinal ones) is consistent with the Q^2-behaviour of the data starting already at $Q^2 \simeq 1\ (GeV/c)^2$.

Basing on naive counting arguments (see, e.g., Ref. [40]), one can argue that the twist expansion for the transverse moments at $Q^2 \simeq \mu^2$ can be approximately rewritten as

$$M_n^T(\mu^2) \simeq A_n^{(2)} \left[1 + n \left(\frac{\Gamma_n^{(4)}}{\mu} \right)^2 - n^2 \left(\frac{\Gamma_n^{(6)}}{\mu} \right)^4 \right] \tag{36}$$

where $A_n^{(2)}$ is the twist-2 contribution and $\Gamma_n^{(4)}$ ($\Gamma_n^{(6)}$) represents the mass scale of the twist-4 (twist-6) term, expected to be approximately independent of n for $n \gtrsim 4$. (Note that in Eq. (36) we have already taken into account the opposite signs of the twist-4 and twist-6 terms as resulting from our analyses). Thus, one gets

$$\Gamma_n^{(4)} = \mu \sqrt{\frac{a_n^{(4)}}{n A_n^{(2)}}} \ , \qquad\qquad \Gamma_n^{(6)} = \mu \left[\frac{|a_n^{(6)}|}{n^2 A_n^{(2)}} \right]^{1/4} . \tag{37}$$

Our results for $\Gamma_n^{(4)}$ and $\Gamma_n^{(6)}$ at $n = 4, 6, 8$, obtained taking $a_n^{(4)}$ and $a_n^{(6)}$ from Tables 6 and 7 and using for $A_n^{(2)}$ the twist-2 term at NLO (i.e., $a_n^{(2)}$) *plus* the whole IR-renormalon contribution (as determined from our fitting procedure and evaluated at $Q^2 = \mu^2 = 1\ (GeV/c)^2$), are collected in Fig. 13. It can clearly be seen that the mass scales of the twist-4 and twist-6 terms are indeed approximately independent of n, viz. $\Gamma_n^{(4)} \simeq \Gamma^{(4)} \simeq 0.76\ GeV$ and $\Gamma_n^{(6)} \simeq \Gamma^{(6)} \simeq 0.55\ GeV$. The value obtained for $\Gamma^{(4)}$ is significantly higher than the naive expectation $\Gamma^{(4)} \simeq \sqrt{< k_\perp^2 >} \simeq 0.3\ GeV$ [40, 41], but not very far from the results of Ref. [13]. Without including the IR-renormalon contribution in $A_n^{(2)}$ (i.e., taking only $A_n^{(2)} = a_n^{(2)}$), the values of $\Gamma^{(4)}$ and $\Gamma^{(6)}$ would increase by $\simeq 20\%$ and $\simeq 10\%$, respectively (cf. also Ref. [42]).

Before closing the Section, we want to address briefly the impact that the specific value adopted for the strong coupling constant at the Z-boson mass can have on our determination of multiparton correlation effects in the transverse channel. As already mentioned, existing analyses of the whole set of DIS (unpolarised) world data favour the value $\alpha_s(M_Z^2) \simeq 0.113$ (see, e.g., Ref. [12]), which is however well below the updated PDG value $\alpha_s(M_Z^2) = 0.119 \pm 0.002$ [23]. Moreover, in Ref. [16] it has been argued that an increase of $\alpha_s(M_Z^2)$ up to $\simeq 0.120$ can give rise to a significative decrease of the relevance of the higher-twists effects in the DIS data (up to a reduction by a factor $\simeq 2$). Therefore, we have repeated our analyses of longitudinal and transverse *pseudo-data* adopting the value $\alpha_s(M_Z^2) = 0.118$, where a set of parton distributions is available from Ref. [43] (we use the parton distributions only for the calculation of $\mu_n^L(Q^2)$ at NLO). All the results obtained at the higher value of $\alpha_s(M_Z^2)$ have the same quality as those presented at $\alpha_s(M_Z^2) = 0.113$ with a slight, but systematic increase of the minima of the χ^2/N variable. The IR-renormalons parameters A_2^{IR} and A_4^{IR} are determined again by fitting the longitudinal data in the Q^2-range from 1 to 20 $(GeV/c)^2$, and their values are now given by $A_2^{IR} \simeq -0.103 \pm 0.017$ and $A_4^{IR} \simeq 0.005 \pm 0.004$, which are compatible within the quoted uncertainties with the corresponding results of the high-Q^2 analysis of Ref. [16]. Thus, by construction, the sum of the twist-2 term at NLO and the

IR-renormalon contribution is almost independent of the specific value of $\alpha_s(M_Z^2)$ in the longitudinal channel. However, the same happens in the transverse channel as it is clearly illustrated in Fig. 14, where the results obtained at $\alpha_s(M_Z^2) = 0.113$ and $\alpha_s(M_Z^2) = 0.118$ are compared in case of the transverse moments with $n \geq 4$ and found to differ only by less than $\simeq 5\%$. Therefore, though the NLO twist-2 terms as well as the IR-renormalon contributions are separately sensitive to the specific value of $\alpha_s(M_Z^2)$, their sum turns out to be quite independent of $\alpha_s(M_Z^2)$. This means that our determination of the multiparton correlation effects is only marginally affected by the specific value adopted for $\alpha_s(M_Z^2)$, at least in the range of values from $\simeq 0.113$ to $\simeq 0.118$.

7 Conclusions

We have analysed the power corrections to the Q^2 behaviour of the low-order moments of both the longitudinal and transverse structure functions of proton and deuteron using available phenomenological fits of existing data in the Q^2 range between 1 and 20 $(GeV/c)^2$. The $SLAC$ proton data of Ref. [3], which cover the region beyond $x \simeq 0.7$ up to $x \simeq 0.98$, as well as existing data in the nucleon-resonance regions have been included in the analysis with the aim of determining the effects of target-dependent higher-twists (i.e., multiparton correlations).

The Natchmann definition of the moments has been adopted for disentangling properly kinematical target-mass and dynamical higher-twist effects in the data. The leading twist has been treated at the NLO in the strong coupling constant and, as far as the transverse channel is concerned, the twist-2 has been extracted simultaneously with the higher-twist terms. The effects of higher orders of the perturbative series have been estimated adopting the infrared renormalon model of Ref. [14], containing both $1/Q^2$ and $1/Q^4$ power-like terms. It has been shown that the longitudinal and transverse data cannot be explained simultaneously by the renormalon contribution only; however, in the whole Q^2 range between 1 and 20 $(GeV/c)^2$ the longitudinal channel appears to be consistent with a pure IR-renormalon picture, adopting strengths not inconsistent with those expected in the naive non-abelianization approximation and in nice agreement with the results of a recent analysis [17] of the $CCFR$ data [18] on $xF_3^N(x, Q^2)$. Then, after including the $1/Q^2$ and $1/Q^4$ IR-renormalon terms as fixed by the longitudinal channel, the contributions of multiparton correlations to both the twist-4 and twist-6 terms have been phenomenologically determined in the transverse channel and found to have non-negligible strengths with opposite signs. It has been also checked that our determination of the multiparton correlation effects is only marginally affected by the specific value adopted for $\alpha_s(M_Z^2)$ (at least in the range from $\simeq 0.113$ to $\simeq 0.118$).

An interesting outcome of our analysis is that the extracted twist-2 contribution in the deuteron turns out to be compatible with the enhancement of the d-quark parton distribution recently proposed in Ref. [16].

Let us stress that our analysis is presently limited by: i) the use of phenomenological fits of existing data (i.e., *pseudo-data*), which are required in order to interpolate the structure functions in the whole x-range for fixed values of Q^2, and ii) by the existing large

uncertainties in the determination of the L/T ratio $R^N_{L/T}(x, Q^2)$. Therefore, both transverse data with better quality at $x \gtrsim 0.6$ and $Q^2 \lesssim 10\ (GeV/c)^2$ and more precise and systematic determinations of the L/T cross section ratio, which may be collected at planned facilities like, e.g., $JLAB$ @ $12\ GeV$, could help to improve our understanding of the non-perturbative structure of the nucleon. Finally, we want to point out that, since in inclusive data multi-parton correlations appear to generate power-like terms with opposite signs, seminclusive or exclusive experiments might offer the possibility to achieve a better sensitivity to individual non-perturbative power corrections.

Acknowledgments

One of the author (S.S.) gratefully acknowledges Stefano Forte for many useful discussions about renormalons and power corrections during the progress of the paper.

References

[1] E.V. Shuryak and A.I. Vainshtein: Nucl. Phys. **B199** (1982) 451; *ib.* **B201** (1982) 141.

[2] A. Bodek et al.: Phys. Rev. **D20** (1979) 7. S. Stein et al.: Phys. Rev. **D12** (1975) 1884.

[3] P. Bosted et al.: Phys. Rev. **D49** (1994) 3091.

[4] European Muon Collaboration, J.J. Aubert et al.: Nucl. Phys. **B259** (1985) 189; *ib.* **B293** (1987) 740.

[5] $BCDMS$ Collaboration: A.C. Benvenuti et al.: Phys. Lett. **B223** (1989) 485; *ib.* **B237** (1990) 592.

[6] New Muon Collaboration, M. Arneodo et al.: Nucl. Phys. **B483** (1997) 3197; *ib.* **B487** (1997) 3.

[7] L.W. Whitlow et al.: Phys. Lett. **B282** (1992) 475.

[8] SMC Collaboration, B. Adeva et al.: Phys. Rev. **D58** (1998) 112001.

[9] $CDHS$ Collaboration, A. Abramowicz et al.: Phys. Lett. **B107** (1981) 141. $CDHSW$ Collaboration, P. Berge et al.: Z. Phys. **C49** (1991) 187. S. Dasu et al.: Phys. Rev. **D49** (1994) 5641. $E140X$ Collaboration : L.H. Tao el al.: Z. Phys. **C70** (1996) 387.

[10] L.W. Whitlow et al.: Phys. Lett. **B250** (1990) 193.

[11] J. Bartelski et al.: e-print archive hep-ph/9804415.

[12] M. Virchaux and A. Milsztajn: Phys. Lett. **B274** (1992) 221.

[13] X. Ji and P. Unrau: Phys. Rev. **D52** (1995) 72.

[14] M. Dasgupta and B.R. Webber: Phys. Lett. **B382** (1996) 273.

[15] E. Stein et al.: Phys. Lett. **B376** (1996) 177. M. Maul et al.: Phys. Lett. **B401** (1997) 100.

[16] U.K. Yang and A. Bodek: Phys. Rev. Lett. **82** (1999) 2467.

[17] A.V. Sidorov and M.V. Tokarev: Nuovo Cim. **110A** (1997) 1401. A.L. Kataev et al.: e-print archive hep-ph/9809500.

[18] $CCFR-NuTev$ Collaboration, W.G. Seligman et al.: Phys. Rev. Lett. **79** (1997) 1213.

[19] G. Ricco et al.: Phys. Rev. **C57** (1998) 356; Few-Body Syst. Suppl. **10** (1999) 423.

[20] H.D. Politzer: Phys. Rev. Lett. **30** (1973) 1346. D.J. Gross and F. Wilczek: Phys. Rev. Lett. **30** (1973) 1323. See also F.J. Yndurain: *The Theory of Quark and Gluon Interactions*, Springer Verlag (New York, 1993).

[21] G. Altarelli: Phys. Rept. **81** (1982) 1.

[22] O. Natchmann: Nucl. Phys. **B63** (1973) 237.

[23] Paritcle Data Group, C. Caso et al.: Eur. Phys. J. **C3** (1998) 1.

[24] V. Burkert: preprint CEBAF-PR-93-035.

[25] L.M. Stuart et al.: Phys. Rev. **D58** (1998) 032003.

[26] C. Ciofi degli Atti and S. Simula: Phys. Lett. **B325** (1994) 276; Phys. Rev. **C53** (1996) 1689.

[27] M. Anghinolfi et al.: Nucl. Phys. **A602** (1996) 405. See also M. Anghinolfi et al.: J. Phys. G: Nucl. Part. Phys. **21** (1995) L9.

[28] M. Lacombe et al.: Phys. Rev. **C21** (1980) 861.

[29] A. Lung et al.: Phys. Rev. Lett. **70** (1993) 718.

[30] M. Okawa: Nucl. Phys. **172** (1980) 481; *ibid.* **B187** (1981) 71.

[31] R.L. Jaffe and M. Soldate: Phys. Lett. **B105** (1981) 467.

[32] M. Glück, E. Reya and A. Vogt: Z. Phys. **C67** (1995) 433.

[33] J. Gomez et al.: Phys. Rev. **D49** (1994) 4348.

[34] See for a recent review about renormalons, M. Beneke: preprint CERN-TH/98-233, July 1998 (e-print archive hep-ph/9807443), and references therein quoted.

[35] I.I. Balitsky and V.M. Braun: Nucl. Phys. **B311** (1988/89) 541.

[36] Yu.L. Dokshitzer, G. Marchesini and B.R. Webber: Nucl. Phys. **B469** (1996) 93.

[37] M. Beneke, V.M. Braun and L. Magnea: Nucl. Phys. **B497** (1997) 297.

[38] V.M. Braun: in Proc. of the XXX^{th} Rencontres de Moriond *QCD and High Energy Hadron Interaction*, Les Arcs (France), March 1995, e-print archive hep-ph/9505317.

[39] E. Stein, M. Maul, L. Mankiewicz and A. Schafer: Nucl. Phys. **B536** (1998) 318.

[40] A. De Rujula, H. Georgi and H.D. Politzer: Ann. Phys. **103** (1977) 315.

[41] R.K. Ellis, W. Furmanski and R. Petronzio: Nucl. Phys. **B212** (1983) 29.

[42] G. Ricco and S. Simula: in Proc. of the Int'l Workshop on *JLAB: Physics and Instrumentation with 6-12 GeV Beams*, Jefferson Laboratory (Newport News, USA), June 1998, JLab Press (Newport News, 1999), p. 313 (also e-print archive hep-ph/9809264).

[43] A.D. Martin, R.G. Roberts, W.J. Stirling and R.S. Thorne: Eur. Phys. J. **C4** (1998) 463. See also A.D. Martin, R.G. Roberts and W.J. Stirling: Phys. Lett. **B387** (1996) 419.

TABLES

Table 1. Values of the twist-2 parameters $a_2^{NS} \equiv \mu_2^{NS}(\mu^2)$, $a_2^S \equiv \mu_2^S(\mu^2)$ and $a_2^G \equiv \mu_2^G(\mu^2)$, and of the twist-4 parameters $a_2^{(4)}$ and $\gamma_2^{(4)}$, obtained by fitting with Eq. (23) the pseudo-data for the proton and the deuteron (see Figs. 2(a) and 3(a), respectively). In case of the proton the parameters a_2^S and a_2^G have been kept fixed at the values obtained for the deuteron. The last row reports the value of the χ^2 of the fit divided by the number of degrees of freedom.

Table 1

parm	*deuteron*	*proton*
a_2^{NS}	0.067 ± 0.014	0.092 ± 0.007
a_2^S	0.112 ± 0.015	0.112
a_2^G	0.066 ± 0.040	0.066
$a_2^{(4)}$	$\lesssim 10^{-4}$	0.012 ± 0.010
$\gamma_2^{(4)}$	—-	1 ± 1
χ^2/N	0.11	0.10

Table 2. Values of the twist-2 parameter $a_n^{(2)}$ and of the higher-twist parameters $a_n^{(4)}$, $\gamma_n^{(4)}$, $a_n^{(6)}$ and $\gamma_n^{(6)}$, obtained by fitting with Eq. (24) the proton pseudo-data of Fig. 2 for $n = 4, 6$ and 8. The last row reports the value of the χ^2 of the fit divided by the number of degrees of freedom.

Table 2

parm	*proton*		
	M_4^T	M_6^T	M_8^T
$a_n^{(2)}$	0.028 ± 0.001	0.0078 ± 0.0003	0.0030 ± 0.0001
$a_n^{(4)}$	0.071 ± 0.009	0.046 ± 0.003	0.029 ± 0.003
$\gamma_n^{(4)}$	3.8 ± 0.4	3.7 ± 0.2	3.6 ± 0.2
$a_n^{(6)}$	-0.056 ± 0.008	-0.039 ± 0.005	-0.026 ± 0.002
$\gamma_n^{(6)}$	2.5 ± 0.5	2.3 ± 0.2	2.1 ± 0.4
χ^2/N	0.05	0.27	0.65

Table 3. The same as in Table 2, but for the deuteron.

Table 3

parm	*deuteron*		
	M_4^T	M_6^T	M_8^T
$a_n^{(2)}$	0.022 ± 0.001	0.0060 ± 0.0002	0.0024 ± 0.0001
$a_n^{(4)}$	0.055 ± 0.006	0.036 ± 0.004	0.022 ± 0.002
$\gamma_n^{(4)}$	3.9 ± 0.2	4.0 ± 0.2	3.8 ± 0.3
$a_n^{(6)}$	-0.046 ± 0.005	-0.032 ± 0.004	-0.020 ± 0.002
$\gamma_n^{(6)}$	2.5 ± 0.2	2.4 ± 0.2	2.2 ± 0.5
χ^2/N	0.10	0.37	1.0

Table 4. Values of the IR-renormalon parameters A_2^{IR} and A_4^{IR} obtained using Eq. (33) to fit the longitudinal proton data of Fig. 4. The twist-2 contribution $\mu_n^L(Q^2)$ is calculated at NLO via Eq. (12) adopting the GRV set of parton distributions [32], while $\mu_n^T(Q^2)$ (see Eq. (9)) is obtained using the values of $a_n^{(2)}$ reported in Table 2. The last row reports the value of the χ^2 of the fit divided by the number of degrees of freedom.

Table 4

parm	*proton*			
	M_2^L	M_4^L	M_6^L	M_8^L
A_2^{IR}	-0.16 ± 0.05	-0.12 ± 0.04	-0.11 ± 0.04	-0.13 ± 0.04
A_4^{IR}	0.06 ± 0.03	0.01 ± 0.01	-0.001 ± 0.001	0.0004 ± 0.0004
χ^2/N	0.24	1.5	1.1	0.42

Table 5. The same as in Table 4, but for the deuteron.

Table 5

parm	*deuteron*			
	M_2^L	M_4^L	M_6^L	M_8^L
A_2^{IR}	-0.18 ± 0.06	-0.14 ± 0.04	-0.14 ± 0.04	-0.15 ± 0.01
A_4^{IR}	0.06 ± 0.03	0.025 ± 0.013	0.012 ± 0.008	0.009 ± 0.003
χ^2/N	0.09	0.26	0.36	0.18

Table 6. Values of the twist-2 parameter $a_n^{(2)}$ and of the higher-twist parameters $a_n^{(4)}$, $\gamma_n^{(4)}$, $a_n^{(6)}$ and $\gamma_n^{(6)}$, obtained by fitting with Eq. (35) the proton pseudo-data of Fig. 2 for $n = 4, 6$ and 8. The IR-renormalon twist-4 and twist-6 contributions are obtained using $A_2^{IR} = -0.132\ GeV^2$ and $A_4^{IR} = 0.009\ GeV^4$ (see text). The last row reports the value of the χ^2 of the fit divided by the number of degrees of freedom.

Table 6

parm	*proton*		
	M_4^T	M_6^T	M_8^T
$a_n^{(2)}$	0.028 ± 0.001	0.0079 ± 0.0003	0.0031 ± 0.0001
$a_n^{(4)}$	0.061 ± 0.008	0.045 ± 0.002	0.028 ± 0.003
$\gamma_n^{(4)}$	4.1 ± 0.2	4.1 ± 0.2	4.1 ± 0.5
$a_n^{(6)}$	-0.051 ± 0.008	-0.041 ± 0.002	-0.027 ± 0.003
$\gamma_n^{(6)}$	2.7 ± 0.2	2.6 ± 0.2	2.4 ± 0.2
χ^2/N	0.06	0.21	0.66

Table 7. The same as in Table 6, but for the deuteron.

Table 7

parm	*deuteron*		
	M_4^T	M_6^T	M_8^T
$a_n^{(2)}$	0.022 ± 0.001	0.0060 ± 0.0002	0.0024 ± 0.0001
$a_n^{(4)}$	0.047 ± 0.004	0.032 ± 0.003	0.020 ± 0.002
$\gamma_n^{(4)}$	4.4 ± 0.2	4.2 ± 0.2	4.1 ± 0.3
$a_n^{(6)}$	-0.043 ± 0.003	-0.030 ± 0.003	-0.019 ± 0.002
$\gamma_n^{(6)}$	2.9 ± 0.2	2.6 ± 0.2	2.4 ± 0.3
χ^2/N	0.10	0.37	1.0

FIGURES

DEUTERON

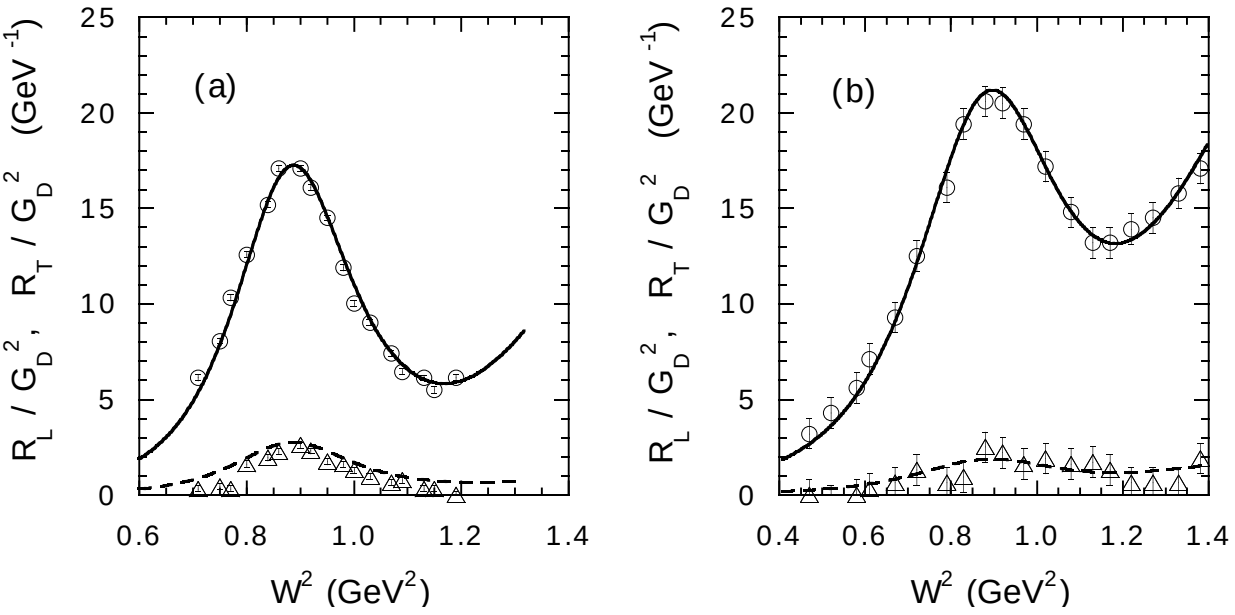

Figure 1. Reduced response functions of the deuteron versus the squared invariant mass $W^2 \equiv M^2 + Q^2 \cdot (1/x - 1)$, measured at *SLAC* [29] for $Q^2 = 1.75$ $(GeV/c)^2$ (a) and $Q^2 = 3.25$ $(GeV/c)^2$ (b). The open dots and triangles correspond to the (reduced) longitudinal R_L and transverse R_T responses, respectively. The solid and dashed lines are the results obtained using the procedure of Ref. [26]. The dipole form factor $G_D(Q^2)$ is explicitly given by $G_D = 1/(1 + Q^2/0.71)^2$.

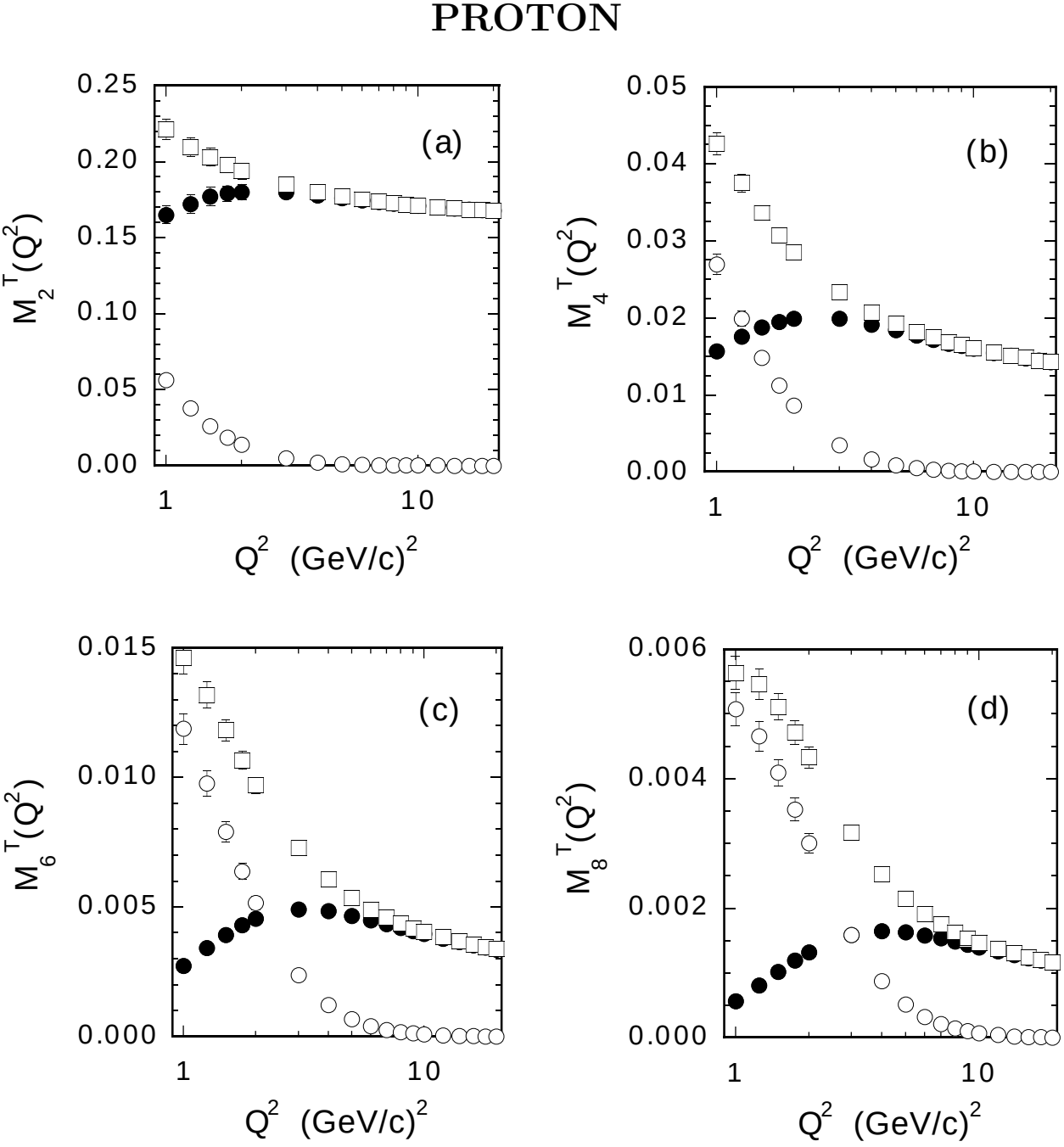

Figure 2. Pseudo-data for the (Natchmann) transverse moments $M_n^T(Q^2)$ (Eq. (13)) of the proton versus Q^2 for $n = 2, 4, 6$ and 8. Open and full dots correspond to the inelastic and elastic contributions, respectively, while the open squares are the total moments. The elastic contribution is evaluated via Eq. (21) assuming a dipole form for the form factors.

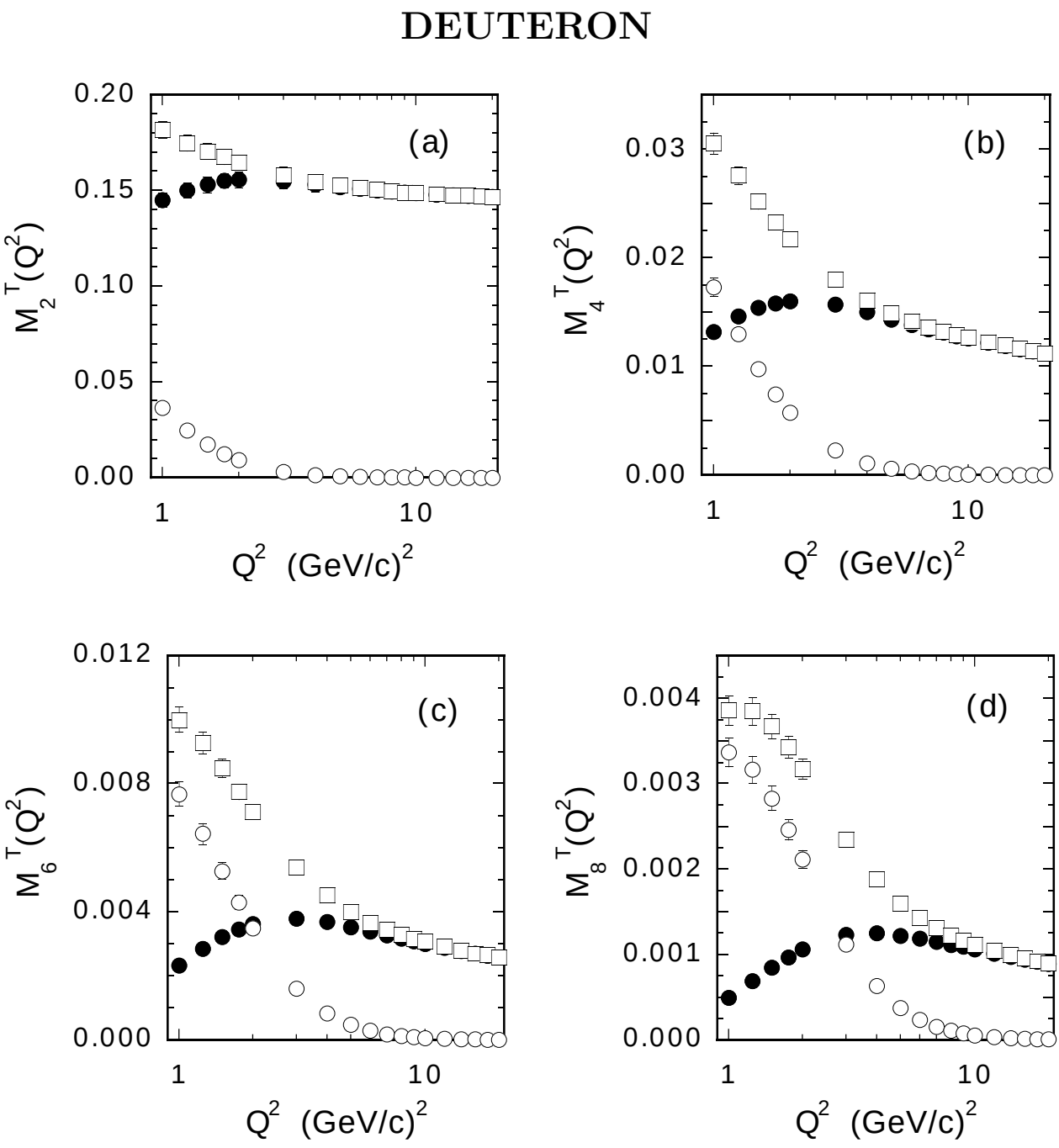

Figure 3. The same as in Fig. 2, but for the deuteron.

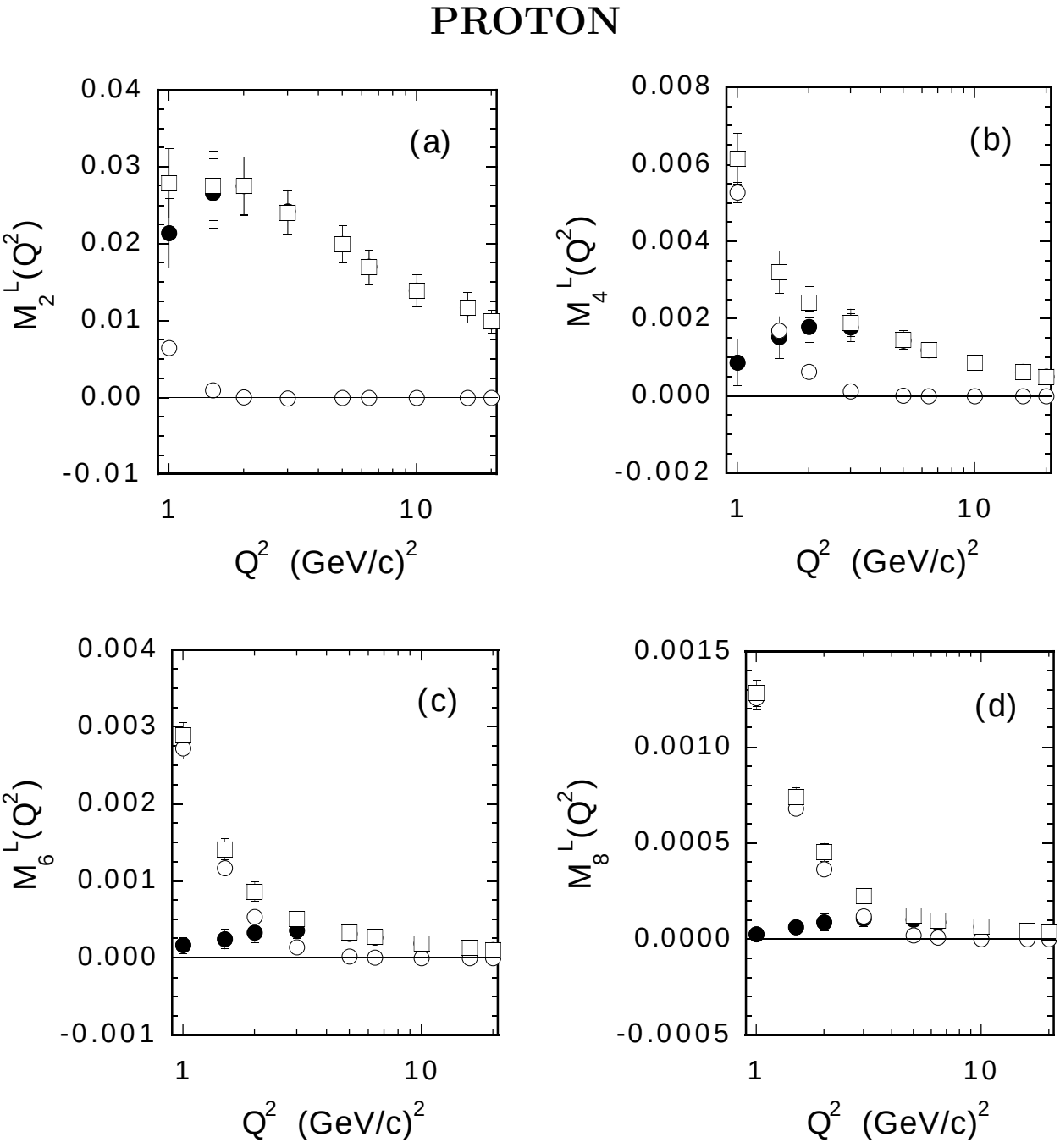

Figure 4. Pseudo-data for the (Natchmann) longitudinal moments $M_n^L(Q^2)$ (Eq. (14)) of the proton versus Q^2 for $n = 2, 4, 6$ and 8. Open and full dots correspond to the inelastic and elastic contributions, respectively, while the open squares are the total moments. The elastic contribution is evaluated via Eq. (22) assuming a dipole form for the form factors.

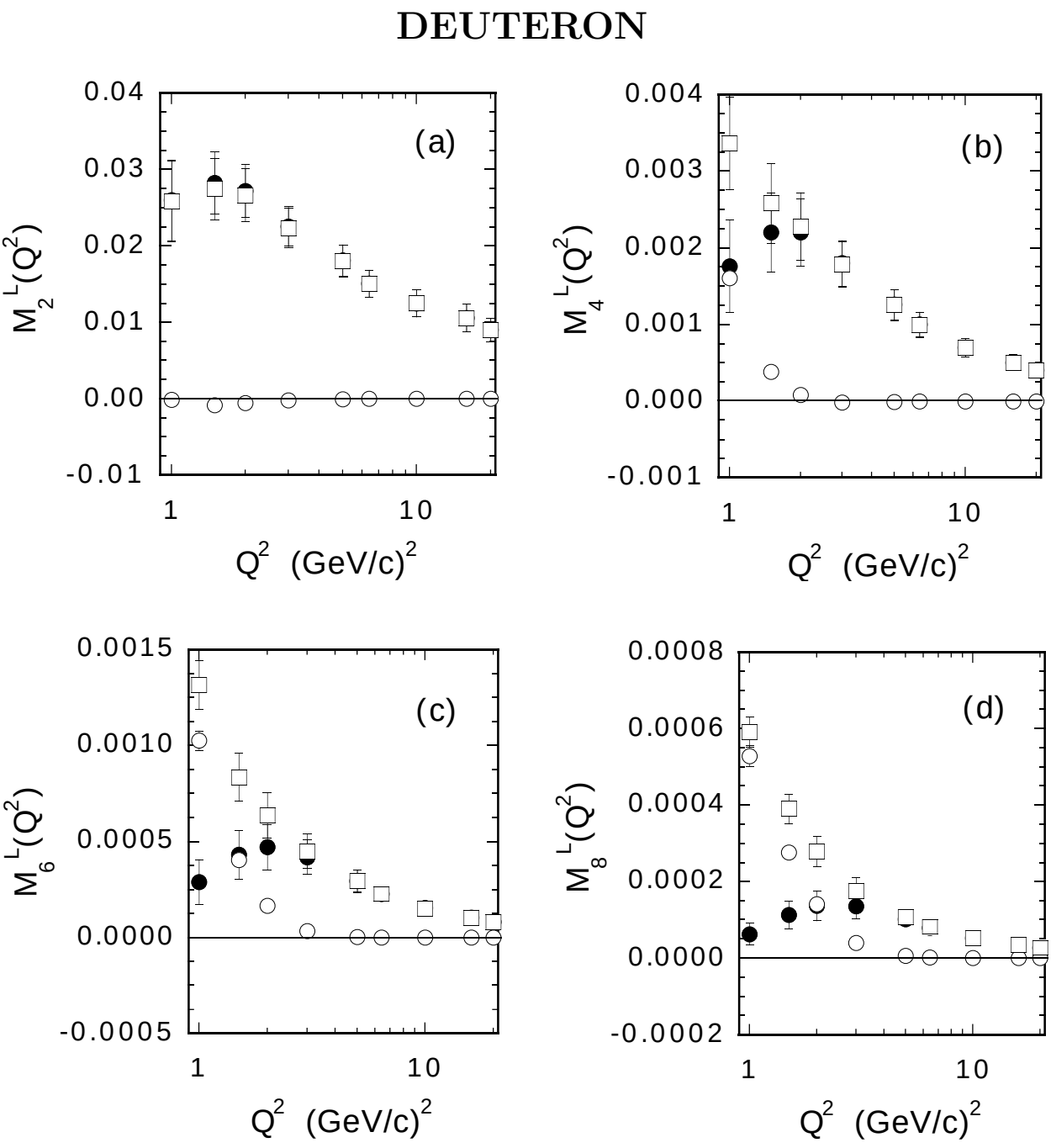

Figure 5. The same as in Fig. 4, but for the deuteron.

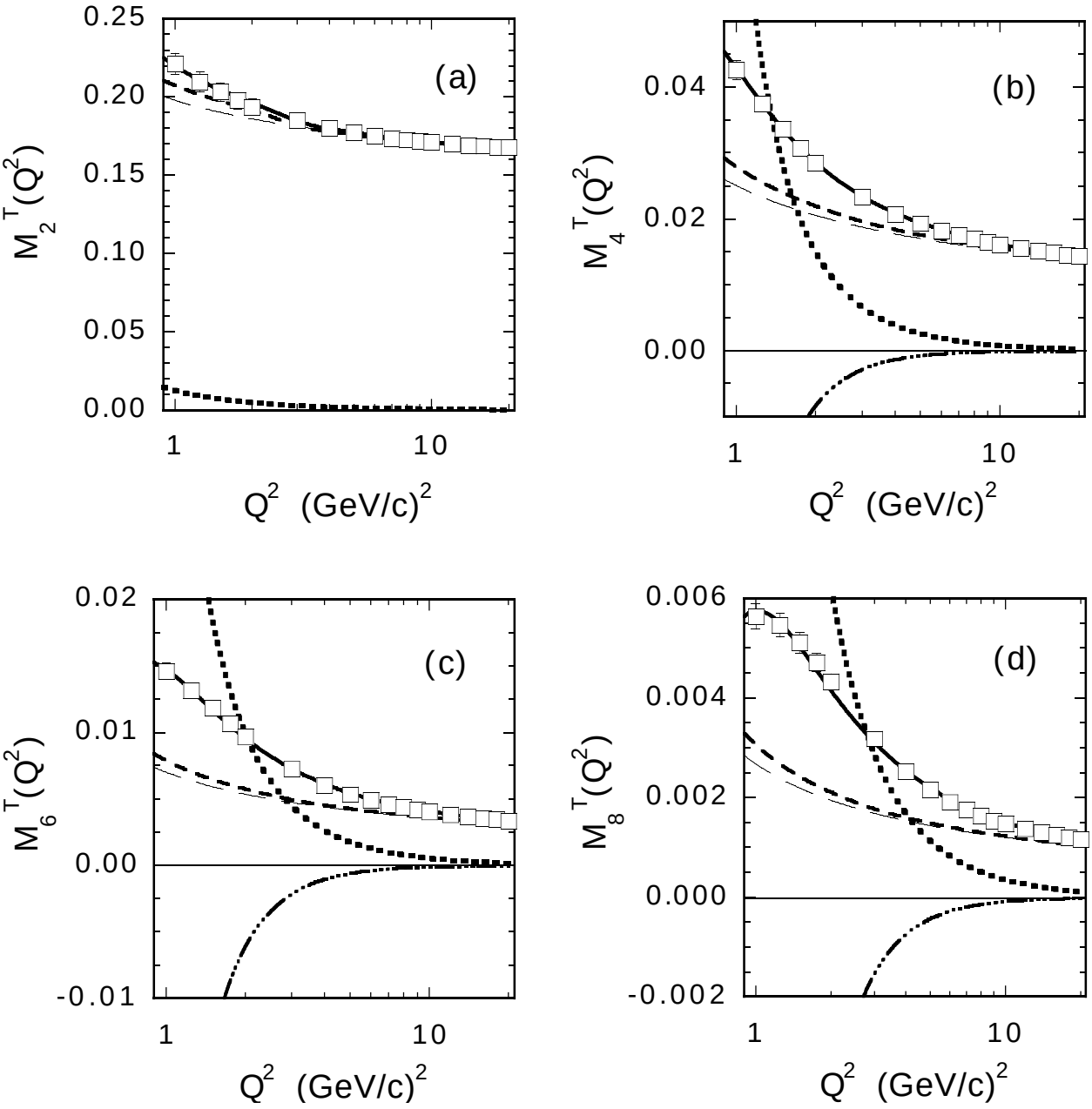

Figure 6. Twist analysis of the proton transverse moments $M_n^T(Q^2)$ (Eq. (13)) for $n = 2, 4, 6$ and 8. The open squares represent the pseudo-data of Fig. 2. The thick solid lines are the result of Eqs. (23) and (24) fitted by the least-χ^2 procedure to the pseudo-data of Fig. 2. The thick dashed, dotted and dot-dashed lines correspond to the contributions of the twist-2, twist-4 and twist-6, respectively. The thin long-dashed lines are the predictions of the twist-2 term obtained using the parton distributions of Ref. [32].

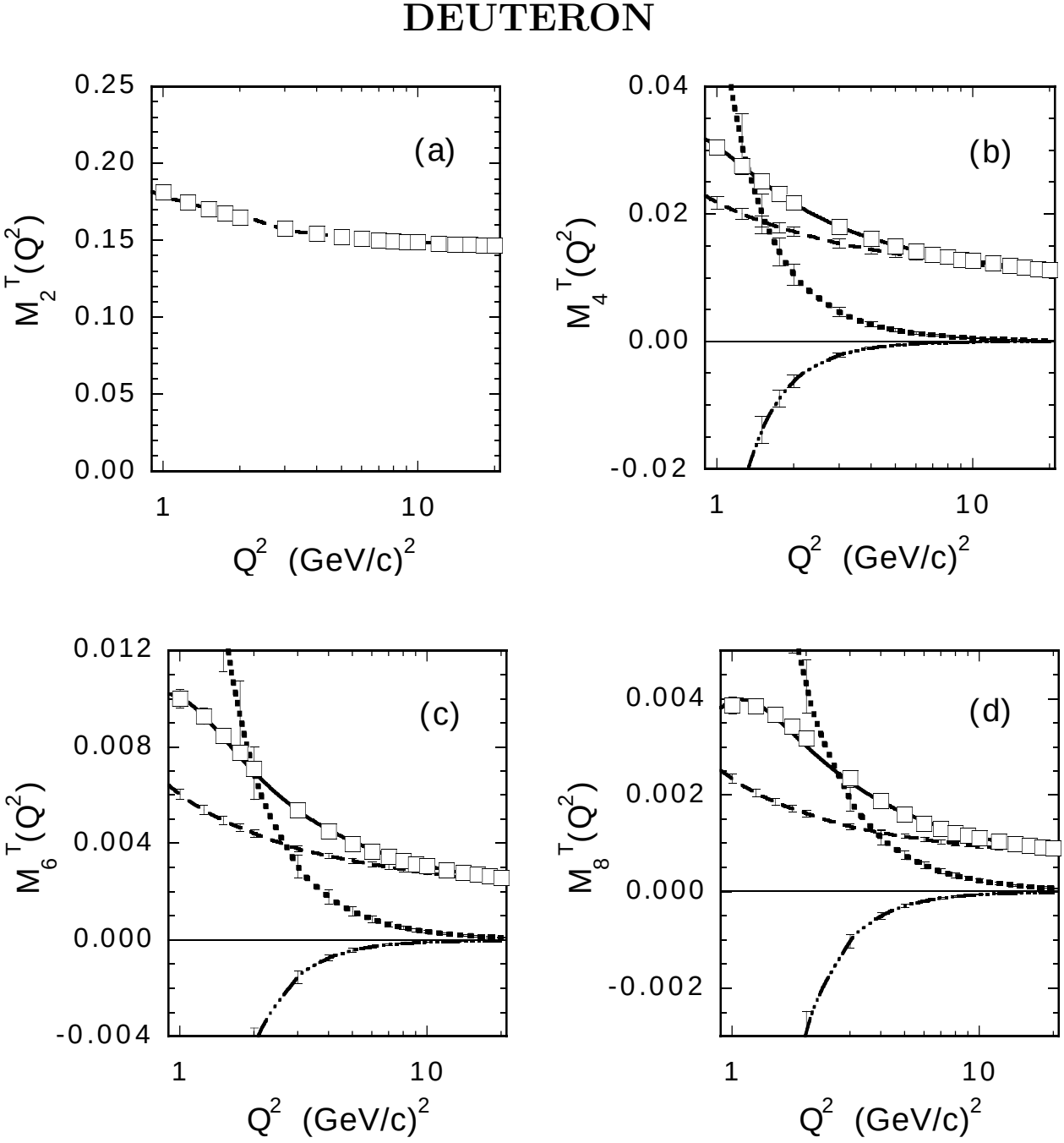

Figure 7. The same as in Fig. 6, but for the deuteron. In (a) only the twist-2 term is reported (see text). In (b), (c) and (d) the error bars on the different twist contributions correspond to the total uncertainties generated by the errors of the parameters appearing in Table 3.

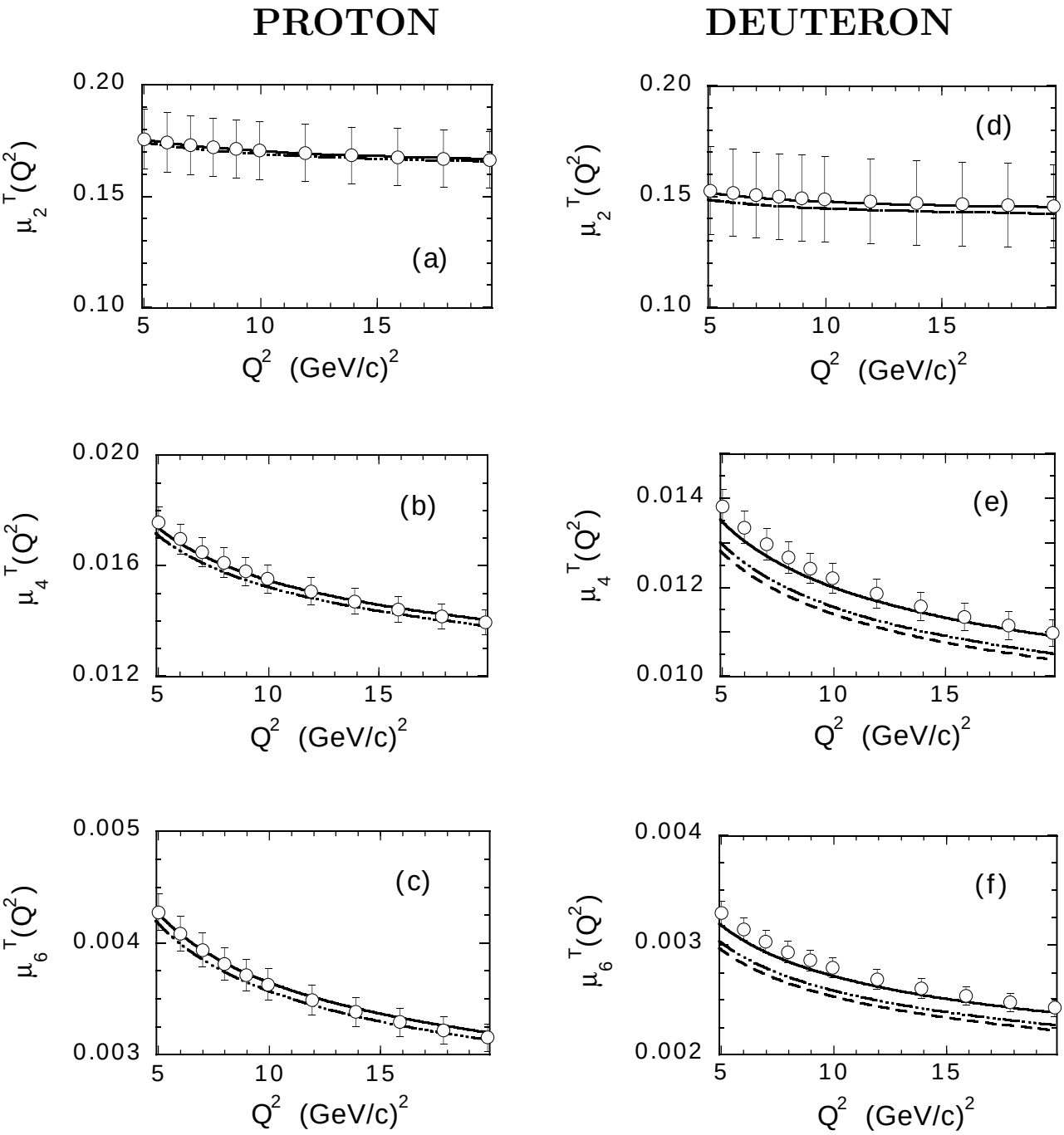

Figure 8. The leading-twist moments $\mu_n^T(Q^2)$ (see Eqs. (4-6)) versus Q^2 for $n = 2, 4, 6$. Open dots: twist-2 extracted from our analysis of the proton and deuteron transverse pseudo-data (see also Tables 1-3); the errors represent the uncertainty of the fitting procedure corresponding to one-unit increment of the χ^2/N variable. Dot-dashed lines: *GRV* prediction at *NLO* [32]. Dashed lines: the same as the dot-dashed lines, but including the empirical nuclear correction of Ref. [33]. Solid lines: the same as the dashed lines, but including the enhancement of the d-quark distribution at large x of Ref. [16], given explicitly by $\tilde{d}(x) = d(x) + 0.1x(1+x)u(x)$.

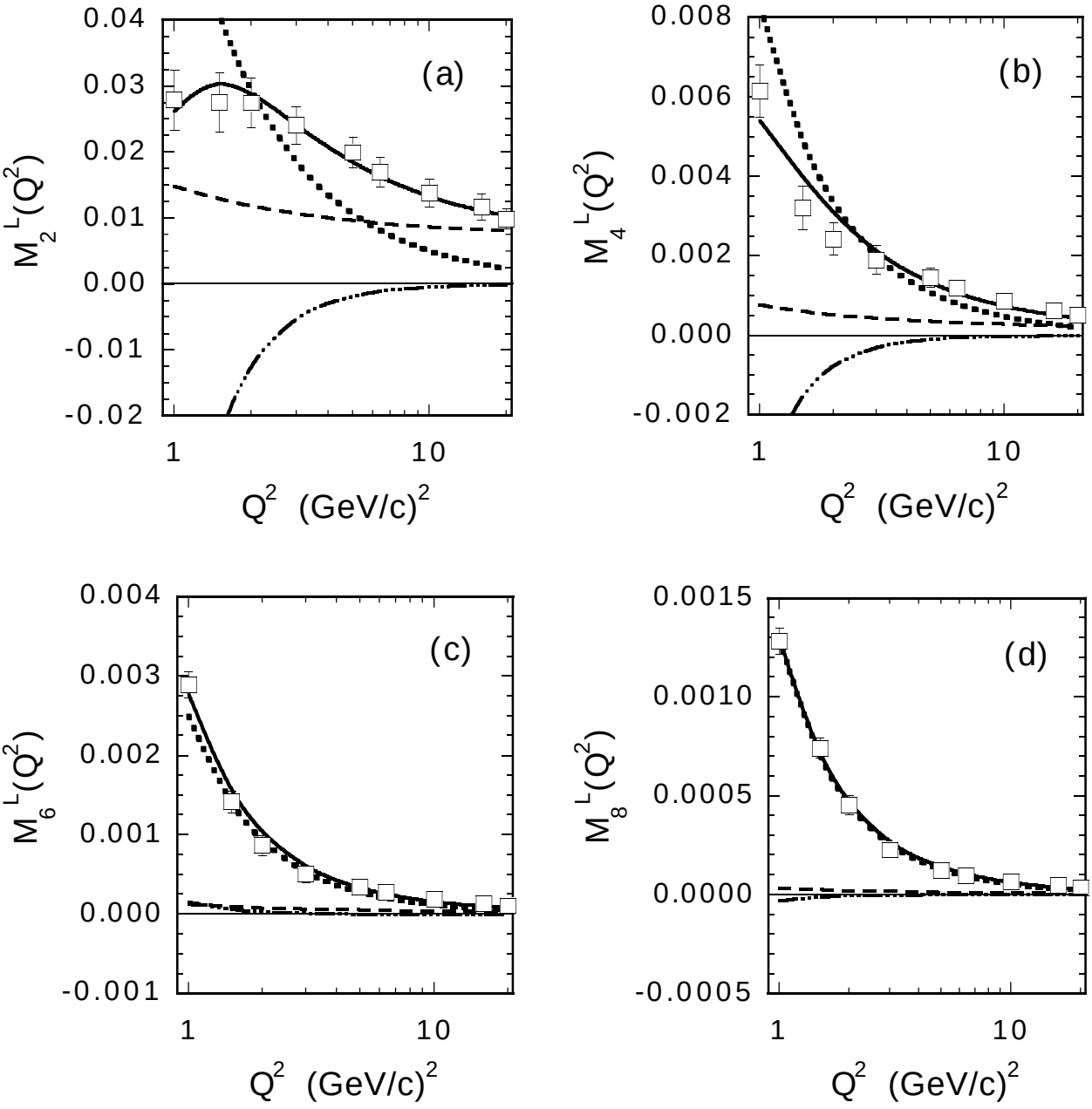

Figure 9. Twist analysis of the proton longitudinal moments $M_n^L(Q^2)$ (Eq. (14)) for $n = 2, 4, 6$ and 8, adopting the IR-renormalon model of Ref. [14]. The open squares represent the pseudo-data of Fig. 7. The solid lines are the results of Eq. (33) fitted by the least-χ^2 procedure to the pseudo-data. The dashed lines are the twist-2 contribution given by Eq. (12) adopting the GRV set of parton distributions [32] at NLO. The dotted and dot-dashed lines correspond to the twist-4 and twist-6 terms, respectively.

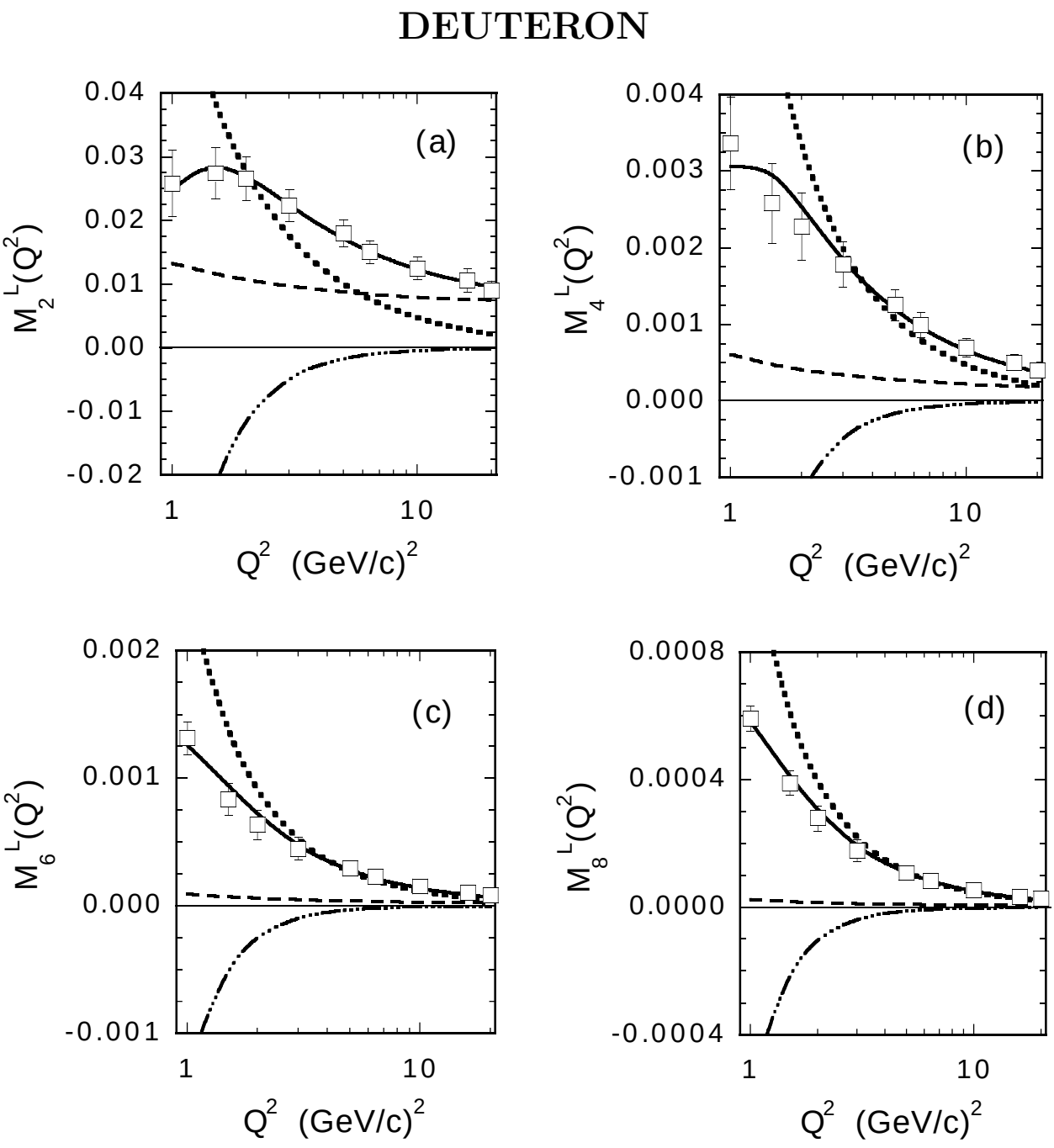

Figure 10. The same as in Fig. 9, but for the deuteron.

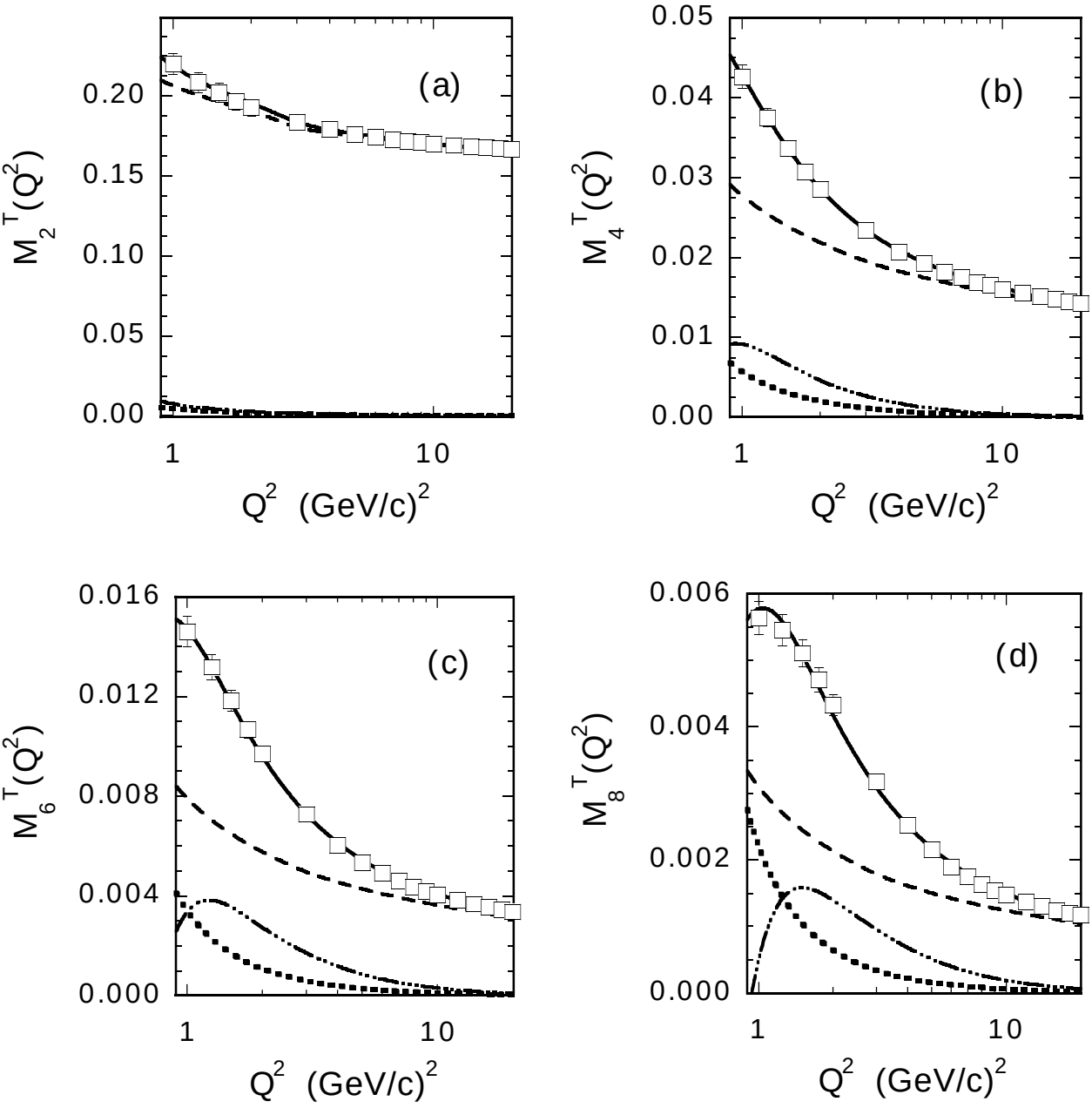

Figure 11. Twist analysis of the proton transverse moments $M_n^T(Q^2)$ (Eq. (13)) for $n = 2, 4, 6$ and 8, including both phenomenological higher twists originating from multiparton correlations and the power corrections arising from the IR-renormalon model of Ref. [14] (see text). The values of the IR-renormalon parameters are fixed at $A_2^{IR} = -0.132\ GeV^2$ and $A_4^{IR} = 0.009\ GeV^4$, as resulting from the analysis of the longitudinal moments. The solid lines are the results of Eq. (34) fitted by the least-χ^2 procedure to the pseudo-data (open squares). The dashed lines are the twist-2 contribution, while the dotted and dot-dashed lines correspond to the IR-renormalon and multiparton correlation contributions, respectively.

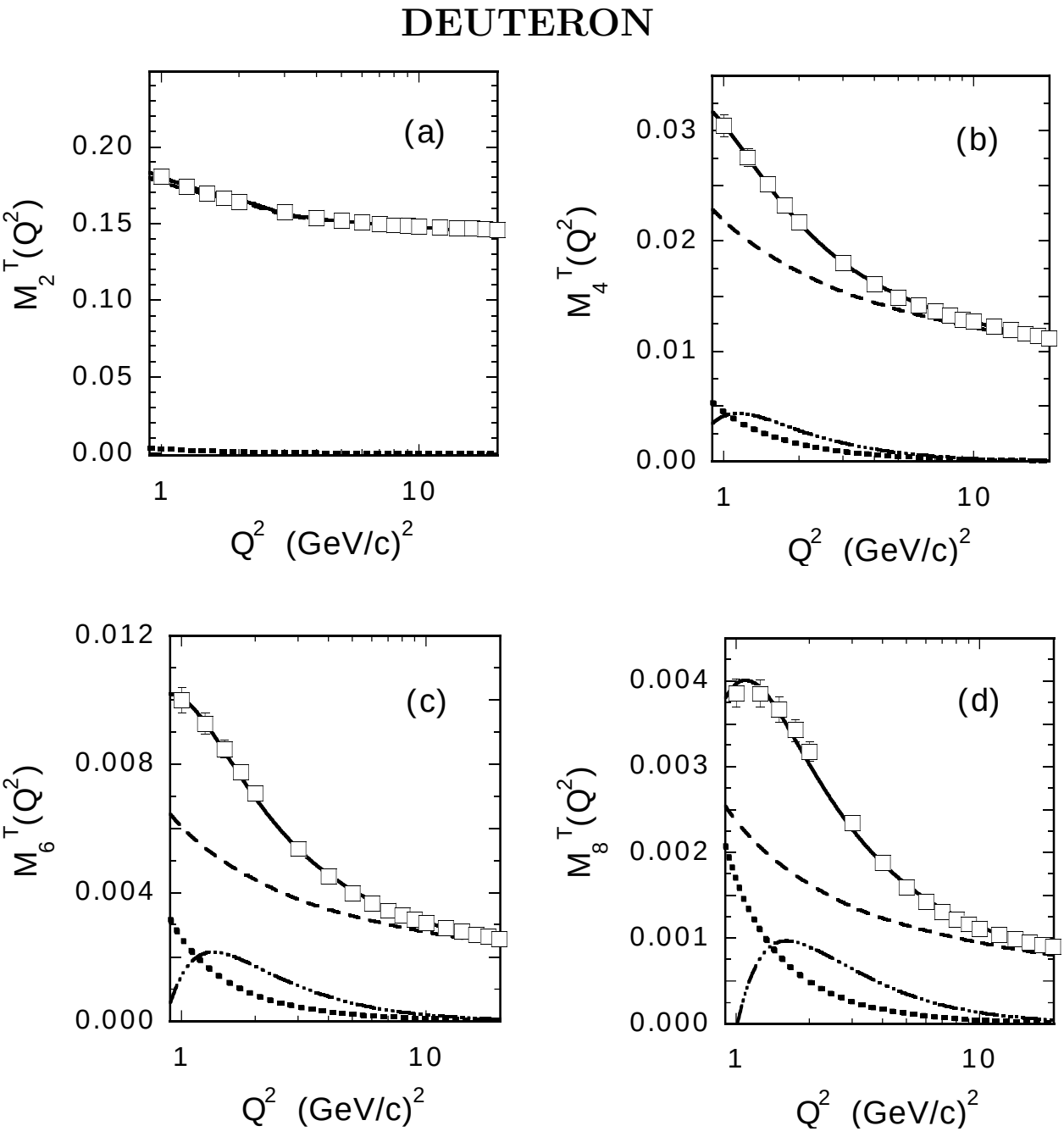

Figure 12. The same as in Fig. 11, but for the deuteron. In (a) only the twist-2 term and the IR-renormalon contribution are reported (see text).

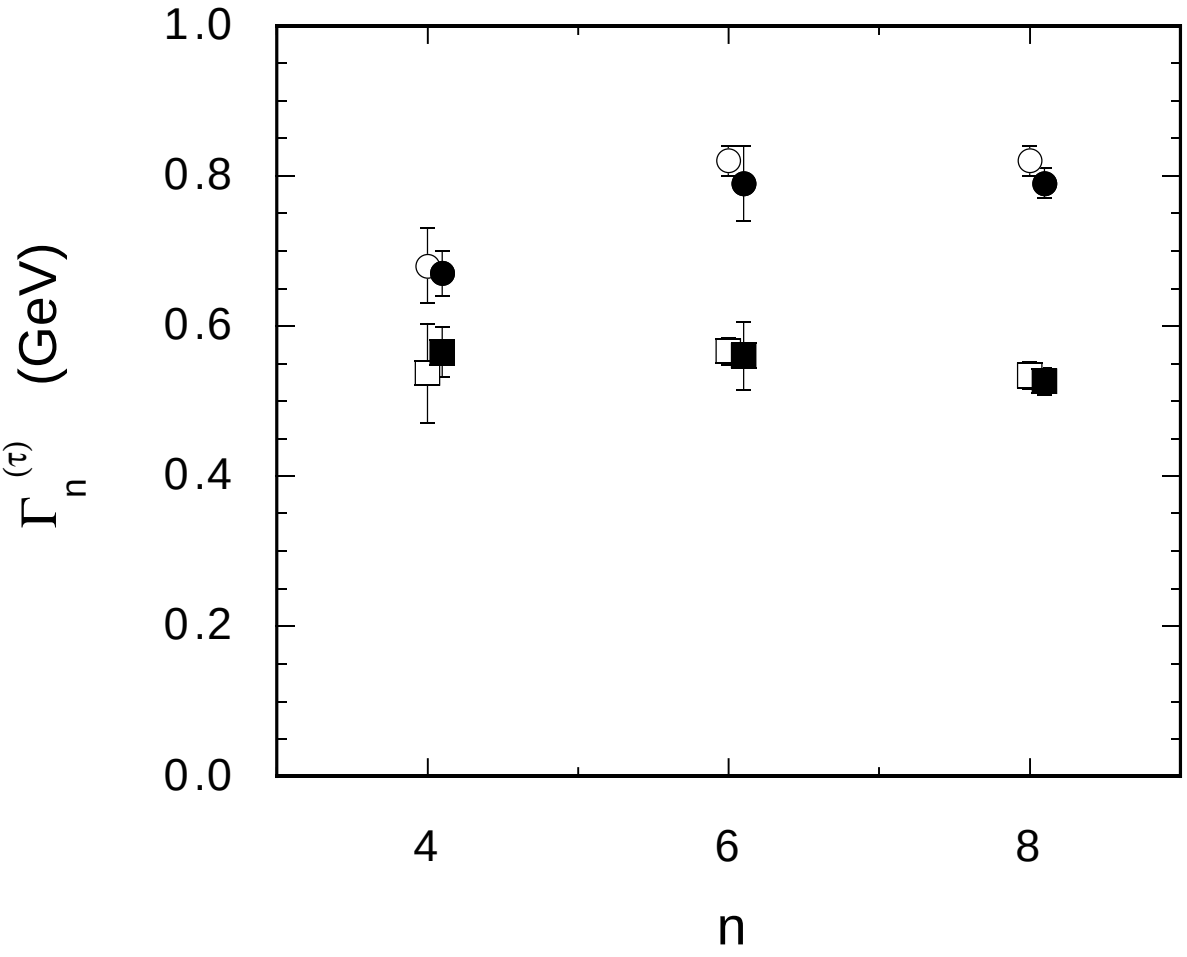

Figure 13. The mass scale $\Gamma_n^{(\tau)}$ (see Eq. (37)) of the twist-4 and twist-6 terms resulting from our final analysis of the transverse pseudo-data (see Tables 6 and 7). Open and full markers correspond to the proton and deuteron case, while dots and squares are our results for the twist-4 and twist-6, respectively (see text).

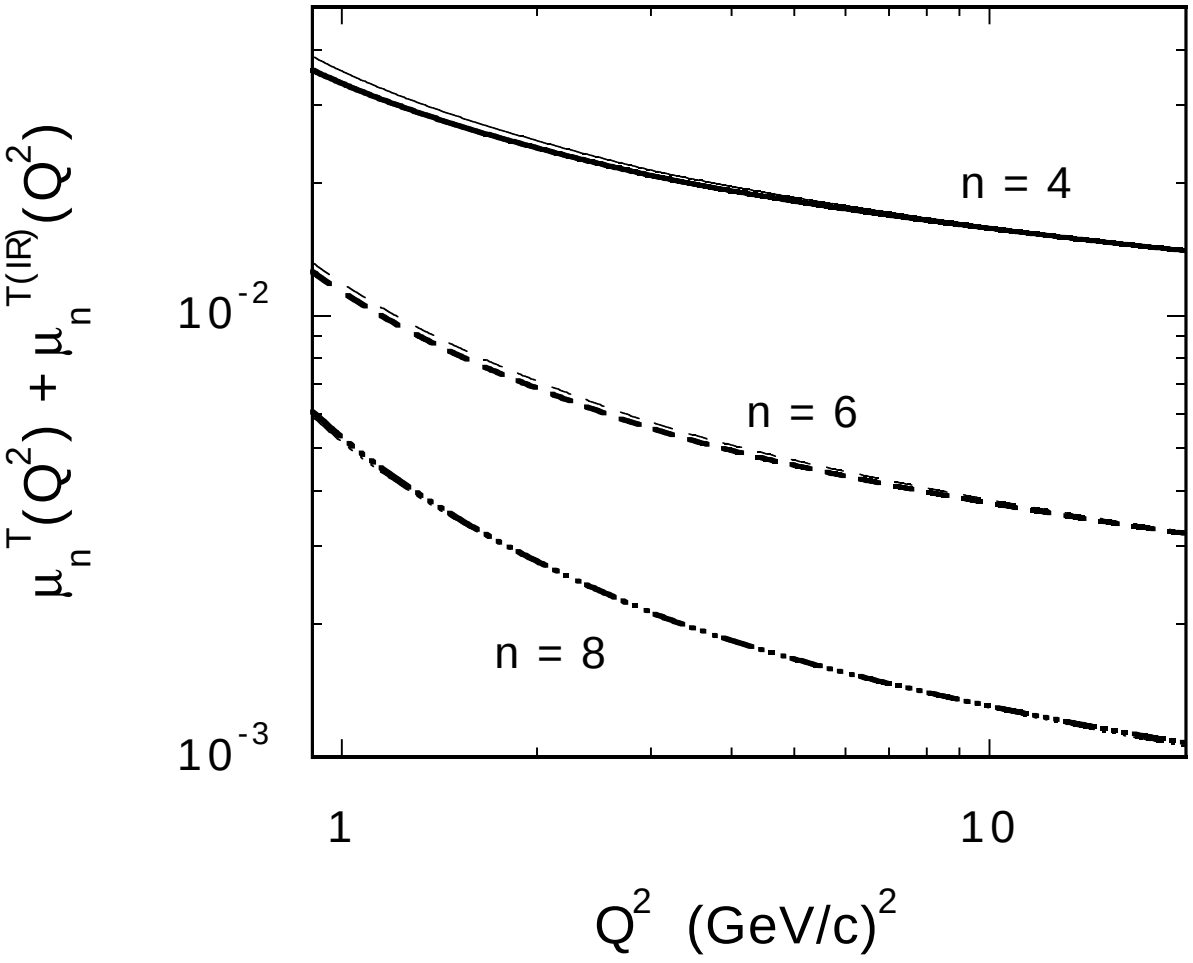

Figure 14. The sum of the NLO twist-2 (Eq. (9)) and the IR-renormalon (Eq. (27)) contributions to the transverse moments $M_n^T(Q^2)$ with $n \geq 4$, as extracted from our final analysis of the transverse pseudo-data (see text), versus Q^2. Thin and thick lines are the results obtained at $\alpha_s(M_Z^2) = 0.113$ and 0.118, respectively, while the solid, dashed and dot-dashed lines correspond to the transverse moments of order $n = 4, 6$ and 8, respectively.